



מכון ויצמן למדע

WEIZMANN INSTITUTE OF SCIENCE

Thesis for the degree  
Doctor of Philosophy

עבודת גמר (תזה) לתואר  
דוקטור לפילוסופיה

Submitted to the Scientific Council of the  
Weizmann Institute of Science  
Rehovot, Israel

מוגשת למועצה המדעית של  
מכון ויצמן למדע  
רחובות, ישראל

By  
**Biana Bernshtein**

מאת  
ביאנה ברנשטיין

מעגלי תקשורת של מקרופג'ים במערכת העיכול עם סביבתם במצבי  
בריאות וחולי

**Communication circuits of intestinal macrophages and their  
environment in the healthy and inflamed gut**

Advisor:  
Steffen Jung

מנחה:  
סטפן יונג

January 2018

טבת תשע"ח

## תקציר

מקרופג'ים במעי שוכנים ברקמת החיבור שנמצאת מתחת לשכבת האפיתל, המפרידה אותם מהאוכלוסייה הגדולה והמגוונת של המיקרוביוטה המאכלסת את חלקו החיצוני של המעי. סביבה מורכבת ולא יציבה זו דורשת תקשורת מדוקדקת ומבוקרת היטב בין תאי הגוף. אנו ביססנו מודל עכברי של דלקת מעי, המבוסס על מחיקה גנטית ספציפית לתאי מקרופג'ים של הגן האחראי לביטוי הרצפטור לאינטרלאוקין 10 (IL10r), אלה עכברי  $Cx3cr1^{Cre}; Il10rd^{fl/fl}$ . מקרופג'ים החסרים את הגן ל-IL10r הם פרו-דלקתיים וגורמים לדלקת מעי חמורה ועצמונית, המחקה את זו של ילדים הנושאים מוטציות בגן המקודד ל-IL10R.

אינטרלאוקין 23 (IL23) הוא ציטוקין מקדם-דלקת המעורב בהתפתחות של דלקות מעי בעכברים כמו גם בבני אדם. מצאנו כי מקרופג'ים שלא מבטאים את הקולטן ל-IL10 מראים רמות שעותק גבוהות של IL23, ובתגובה לכך תאי Th17 כמו גם ILC3 מעלים את רמות הביטוי של אינטרלאוקין 22 (IL22). כיוון שתאי אפיתל הם המגיבים העיקריים ל-IL22, מיפינו את התגובה של תאי האפיתל למקרופג'ים פרו-דלקתיים בשני שלבים של המחלה: דלקת ראשונית – שלב בו טרם נצפו סימני מחלה מובהקים, ודלקת מתקדמת – שלב בו ניכרים סימני מחלה בעכברים. בשני השלבים, מצאנו שינויים משמעותיים במתאר הביטוי של תאי האפיתל בתגובה למקרופג'ים פרו-דלקתיים, שכללו עליה ברמות הביטוי של פפטידים אנטי-חיידיקיים וכמוקינים.

על מנת לבחון האם הציטוקינים IL23 ו-IL22 גורמים למחלה או שרמות הביטוי שלהם עולות בתגובה לדלקת, מחקנו את הגנים המקודדים לציטוקינים הללו בעכברי המודל שלנו. כאשר מחקנו את הגן המקודד ל-IL23 במקרופג'ים שלא מבטאים את הקולטן ל-IL10, סימני המחלה ירדו באופן ניכר, דבר אשר מדגיש את חשיבות הציטוקין IL23 בהתפתחות המחלה. בנוסף, מחיקה של הגן המקודד ל-IL22 מכל תאי הגוף בעכברי המודל שלנו, עיכבה גם היא את הדלקת במעי, ולא החמירה אותה. בנוסף, אנו משתמשים במערכות מחיקה וטרנספר של תאים שפותחו במעבדתנו כדי לבחון באופן מעמיק את יחסי הגומלין בין המקרופג'ים לתאי האפיתל ברקמת המעי. על ידי טרנספר של תאים בעלי גנוטיפים שונים אנו חוקרים את התהליכים התאיים המתרחשים בשלבי ההתפתחות הראשוניים של הדלקת.

## Abstract

Intestinal macrophages reside in the connective tissue underlying the gut epithelium, which separates them from the diverse microbiota populating the gut lumen. This complex and dynamic environment necessitates intimate and precise inter-cellular communication. We established a murine colitis model based on macrophage-restricted Interleukin 10 (Il10) receptor deficiency (*Cx3cr1<sup>Cre</sup>:Il10ra<sup>fl/fl</sup>* mice). Il10r deficient gut macrophages are pro-inflammatory, causing severe spontaneous colitis that resembles the pathology of children carrying IL10R mutations.

Il23 is a pro-inflammatory cytokine known to be involved in the pathogenesis of colitis in both mice and humans. Il10r deficient macrophages display elevated levels of Il23, and in response Th17 cells and ILC3 show up-regulated levels of Il22.

Since epithelial cells are the main sensors of Il22, we profiled the response of epithelial cells to pro-inflammatory macrophages at two stages of the disease: early inflammation prior to overt signs of colitis, and late inflammation with apparent signs of disease. In both early and late stages, epithelial cells displayed an altered gene signature, including up regulation of anti-microbial peptides (AMPs) and chemokines indicating an Il22 response.

To examine whether Il23 and Il22 are induced by the colitis or important for colitis initiation, we specifically abolished each of these cytokines in our mouse model.

Interestingly, ablation of macrophage-specific Il23 expression in *Cx3cr1<sup>Cre</sup>:Il10ra<sup>fl/fl</sup>:Il23a<sup>fl/fl</sup>* mice prevented colitis development highlighting this cytokine as critical driver of the disease. Moreover, systemic Il22 ablation, rather than exacerbating inflammation, ameliorated disease development. We further dissect the specific cell types participating in the initiation of the inflammatory process, using a variety of transgenic mice and cell transfer models.

## Table of contents

Title.....	1
Abstract in Hebrew.....	2
Abstract in English.....	3
Table of contents.....	4
Acknowledgments.....	5
Introduction.....	6-10
<b>Part 1 - IL10Ra-deficient macrophages elicit IL23- and IL22-driven colitis</b>	
Introduction – Part 1 .....	11-12
Results – Part 1.....	13-26
Discussion– Part 1.....	26-31
<b>Part 2 - Studying macrophage differentiation using a monocyte transfer model</b>	
Introduction – Part 2 .....	31-32
Results – Part 2.....	32-38
Discussion– Part 2.....	39-40
Materials and methods.....	41-44
References.....	44-51

## **Acknowledgments**

I would like to thank all the current and previous members of the Jung laboratory at the Immunology Department. Specifically, Udi Zigmund who guided me through my M.Sc. studies and provided many tools and knowledge. Caterina Curato who helped me throughout my PhD studies, with both technical and spiritual support. Diana Varol, Yonit Lavin and Yochai Wolf for guidance during my first years in the lab. Thanks for superb technical support – Yifat Segal Hayoun and Louise Maor. For helping me with bioinformatics analysis I owe thanks to Eyal David and Jonathan Grozovski. Thanks to Sigalit Boura Chalfon for good advice and fruitful discussion. Finally, for allowing me to perform all these complex experiments and guiding me through them, always open to new ideas, I would like to thank my advisor Prof. Steffen Jung.

Special thanks to my advising committee Prof. Lea Eisenbach and Prof. Shalev Itzkovitz for guidance throughout my studies, and beyond their duties as advisors. These experiments would not be possible without animal care takers at the WIS, namely Beni Siani, Sharon Ovadia, Dalia Vaknin and Ronen Borochove. Thanks to the histology unit and to Prof. Alon Harmelin for their help with histopathological analysis.

Many of the mouse strains used in this research were kindly provided by Eran Elinav's lab at the WIS. Christoph Thaiss from the Elinav lab helped me with many technical and scientific issues.

Finally and most importantly, I would like to thank from the bottom of my heart my parents who always inspired me to dream big.

And lastly the reason it's all worth it – my husband Shmuel, my son Ronnie and my dog Ginnie.

## Introduction

### IBD – in humans and mice

Inflammatory bowel disorders (IBD) include Crohn's disease and Ulcerative colitis, two chronic and relapsing pathologies of the intestinal tract. Crohn's disease affects mostly the ileum and colon, and can also discontinuously involve other parts of the intestine. Ulcerative colitis involves the colon and mostly affects its distal parts, namely the rectum, in un-continuous manner<sup>1</sup>. IBD affect millions of individuals world-wide and are more prevalent in the western world<sup>2</sup>. Extensive Genome Wide Association Studies (GWAS) have revealed 200 genetic loci, which are associated with IBD, and recent high-resolution fine-mapping in large samples has identified statistically convincing causal variants<sup>3</sup>. Moreover, animal IBD models have provided critical mechanistic insights for defined genetic factors causing and contributing to intestinal inflammation<sup>4</sup>, although much remains to be learned.

Over decades of research, many IBD mouse models were established and characterized, here I elaborate on some of the most popular and studied ones, which are relevant for this thesis:

1. Dextran Sodium Sulfate (DSS) model – An acute model in which a chemical reagent is added to the drinking water of the mice and causes disruption of the epithelial barrier of the large intestine<sup>5</sup>. Previous work from our laboratory has emphasized the role of pro inflammatory monocytes in this model, since ablation of these cells ameliorated disease symptoms<sup>6</sup>.
2. T cell transfer model – Mice deficient in B and T cells are adoptively transferred with naïve T cells. In the absence of T regulatory (Treg) cells, the naïve T cells expand and cause severe intestinal inflammation<sup>7</sup>. Upon transfer of unfractionated T cells, including naïve and regulatory cells, colitis is not developed and the mice are healthy<sup>8</sup>.
3. 'CD40 colitis' – Anti-CD40 antibody is injected to T and B cell deficient mice, causing activation of antigen presenting cells (APC). The mice rapidly lose weight, up to 20% within 4 days, and suffer from wasting disease and severe intestinal inflammation<sup>9</sup>.
4. Interleukin 10 (IL10) deficient mice – Although IL10 is an anti-inflammatory cytokine that is produced by diverse types of cells and tissues, the prominent phenotype of mice deficient of IL10 is spontaneous intestinal inflammation<sup>10</sup>.

Unlike the previously described models, IL10<sup>-/-</sup> mice suffer from chronic colonic inflammation, which develops gradually and worsens with time. Nonetheless, the inflammation is not lethal, and the mice can survive for several months under this condition. As mentioned, the phenotype is spontaneous and depends on the microbiome<sup>11</sup>.

Different colitis models are driven by particular cell types and hence involve distinct mechanisms, evident in the severity of the phenotype and dynamics of disease progression. Arguably, human IBD patients are even more diverse and complex, emphasizing the importance of establishment of various murine models mimicking distinct stages and subtypes of Crohn's disease and Ulcerative Colitis.

### The intestinal mucosa cellular composition

Studies in mice have yielded an unprecedented understanding of the cellular composition of the intestinal mucosa, including mononuclear phagocytes<sup>12,13</sup>, adaptive and innate lymphoid cells (ILC)<sup>14</sup>, as well as inter-cellular communication circuits maintaining gut homeostasis<sup>15</sup>, and the impact of microbiota<sup>16</sup> (**Fig1**<sup>17</sup>).

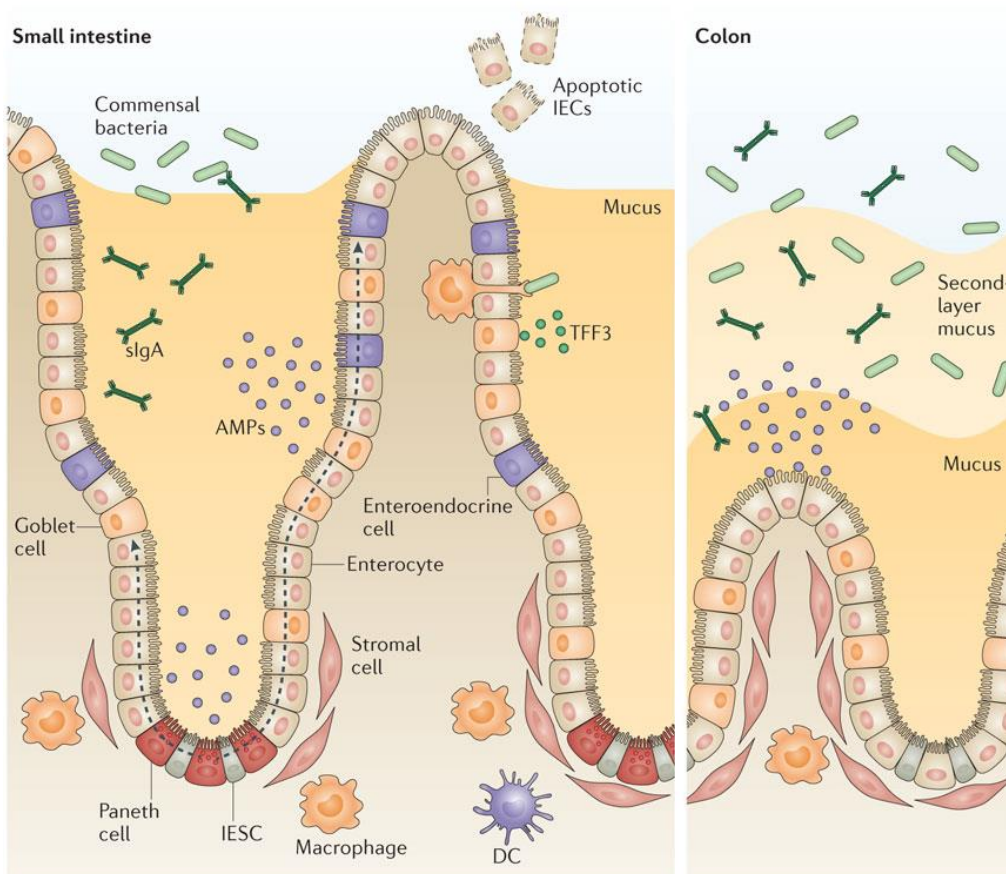


**Figure 1 – Graphical representation of the cellular composition of the small and large intestine. Adapted from Peterson et al, 2014.**

Intestinal macrophages reside in the connective tissue or *lamina propria* underlying the monolayer of epithelial cells (EC). They express the integrins CD11b and CD11c and are readily distinguished from dendritic cells (DC) by their expression of CD64, the high-affinity IgG receptor FcγR, and the chemokine receptor CX<sub>3</sub>CR1<sup>6</sup>. As non-migratory cells, macrophages do not translocate to draining lymph nodes and display limited or no potential to 'prime' naive T cells<sup>18</sup>. In adult mice, the intestinal macrophage compartment was reported to have a half-life of 6-8 weeks<sup>13</sup> and is replenished by infiltrating Ly6C<sup>hi</sup> blood monocytes<sup>19,20</sup>. Monocyte-derived cells replace an embryonically derived population shortly after birth<sup>21</sup>, as opposed to other tissue macrophage compartments that efficiently self-renew throughout adult life<sup>18</sup>. Constant replacement of gut macrophages necessitates continuous adaption of the precursor monocytes to the dynamic gut environment including its prominent constant exposure to microbial stimuli rendering the gut vulnerable<sup>22</sup>.

Dendritic cells (DC) in the small and large intestine are diverse and currently can be divided into several groups according to their expression of CD11b and CD103, as well as XCR1 and SIRPα<sup>13</sup>. XCR1+CD11b-CD103+ present in both the small and large intestine, as well as in lymphoid organs. SIRPα+CD11b+CD103+ DC are more prominent in the small intestine. SIRPα+CD11b-CD103- DC are prominent in the Colon. These three subsets share expression of the transcription factor Zbtb46 and depend on Flt3l for their differentiation. As opposed to macrophages, DC are highly migratory, and serve as the liaison between the *lamina propria* and the mesenteric lymph nodes to ensure conventional T cell immunity and set a homeostatic tone of Th17 and T regulatory cells<sup>23</sup>. For example, intestinal DC express the enzyme retinaldehyde dehydrogenase (ALDH), converting retinal to RA. RA in turn promotes generation of Treg cells in the tissue<sup>24,25</sup>.

Th17 cells are a subset of CD4 T cells, characterized by expression of the receptor-related orphan receptor-γ (RORγt) transcription factor, and produce IL17 and IL22 as signature cytokines<sup>26,27</sup>. Th17 cells have a dual role in immunity: on one hand, they maintain homeostasis by protecting the host against fungal and bacterial infection; on the other hand they were shown to drive several immune pathologies<sup>28</sup>. However, what determines their protective versus pathogenic phenotype is still unclear. Recently, single cell RNA analysis was performed to determine Th17 cell

heterogeneity and potential makers for their pathogenic versus protective phenotype<sup>29,30</sup>. In these two comprehensive studies, *CD51* was found to be expressed in non-pathogenic Th17 cells, whereas *Gpr65* and *Toso* were expressed in pathogenic Th17 cells and were critical for their pro-inflammatory phenotype. Interestingly, alterations in the human *Gpr65* locus are associated with Crohn's disease<sup>31</sup> and IBD<sup>32</sup>.

Innate lymphoid cells (ILC) are defined by their lack of a T cell receptor and dependence on the transcriptional repressor inhibitor of DNA binding 2 (ID2) as well as the common  $\gamma$  chain. ILC reflect hard-wired equivalents of conventional T helper cells, and are in analogy to the latter and their cytokine secretion patterns currently subdivided into three groups<sup>33</sup>. The ILC3 subset depends, like its Th17 equivalent, on the transcription factor ROR $\gamma$ t, and secretes IL-17 and IL-22. IL-22 is critical to maintain gut homeostasis as it is sensed by epithelial cells and participates in wound repair, but also shapes the expression pattern of antimicrobial peptides (AMPs) by enterocytes and Paneth cells. Accordingly, ROR $\gamma$ t deficient mice display impaired AMP expression, as well as abnormalities in the mucus layer structure<sup>34,35</sup>.

The connective tissue harboring the intestinal immune cells, the so-called *lamina propria* is separated from the microbiota by a single tight-junction-sealed epithelial cell layer. However, the intestinal epithelium is not merely a barrier, but rather actively contributes to gut homeostasis by relaying information on the gut content to the deeper tissues. These activities are reflected in a considerable functional specialization of the epithelial cell layer, which comprises five major types of cells. The most abundant intestinal epithelial cells are enterocytes. These cells mainly support nutrient absorption, but can also sense gut lumen content, as indicated by their expression innate immune receptors, such as TLRs<sup>36</sup>. Goblet cells that are more frequent in the large than small intestine, are specialized in mucus secretion, creating a spatial segregation between the luminal microbiota and the epithelial layer<sup>35</sup>. Interestingly, these cells were recently suggested to provide a unique entry port, potentially exploited by entero-pathogens, such as *Listeria monocytogenes*<sup>37,38</sup>. Paneth cells are largely confined to the bottom of the crypts of the small intestine. These cells are specialized in the secretion of sAMPs<sup>39</sup>, but also important for maintenance of the stem cell niche<sup>40</sup>. Epithelial stem cells are a unique subset of cells retaining stem-ness throughout adult life. They are confined to the bottom of each

crypt and continuously give rise to all differentiated subsets of epithelial cells, which have been estimated to have in steady state a half-life of 5 days. Finally, the intestinal epithelium also comprises neuroendocrine cells, a rare type of cells found all along the gastrointestinal tract, that can secrete a large variety of hormones<sup>41</sup>. The epithelial layer provides a critical link between the gut lumen and the underlying immune system, likely informing the latter on the luminal microbiota composition and potential pathogen presence. This feature was recently highlighted by the fact that the unique epithelium-associated commensal called *Segmented Filamentous Bacterium* (SFB), was shown to tune the composition of the intestinal T cell compartment and thereby establish relative resistance to pathogen challenge<sup>42</sup>.

In this thesis I will describe our current progress in understanding the IL10R KO colitis model developed in our laboratory. This colitis model is driven by pro-inflammatory macrophages. In the first part of the thesis I will elaborate on our attempts to decipher the mechanism of colitis induction, using a variety of transgenic mice and advanced flow cytometry and transcriptional profile analysis of distinct cell populations. In the second part I will describe a cell transfer system developed in our laboratory, which allows us to investigate the differentiation process of macrophages in the intestinal tissue context.

# Part 1 - IL10R-deficient macrophages elicit IL23- and IL22-driven colitis

## Introduction – Part 1

### IL10 signaling and IBD

As mentioned, IL10 is an essential molecule maintaining homeostasis of the large intestine. IL10 is monomeric protein and a member of the IL10 cytokine family. It binds to its specific receptor IL10R, a heterodimer of IL10ra and IL10rb. While IL10ra is specific for IL10, IL10rb is shared with other cytokines such as IL22<sup>43,44</sup>. Upon specific binding to its receptor, IL10 propagates a signal through Stat3 phosphorylation. Interestingly, all the components of this signaling pathway have genetic variants associated with IBD<sup>43</sup>. Specifically, children bearing inactivating IL10R mutations were found to succumb to severe early onset gut inflammation<sup>45</sup>. The role of IL10 in maintaining gut homeostasis is conserved among species, since also mice deficient for IL10 develop severe spontaneous colonic inflammation<sup>10</sup>.

Previous work published by our laboratory has focused on the IL10 signaling pathway in colonic macrophages. We have shown that although colonic macrophages produce high levels of IL10 under homeostatic conditions, they are not the critical source of IL10 in the gut<sup>46</sup>. Supportive of this finding, work by other groups suggested that Treg cells are a critical source of IL10<sup>47</sup>. However, we found that IL10 sensing by intestinal macrophages is required for their homeostatic phenotype. Specifically, mice that carry a Cre transgene insertion in their CX<sub>3</sub>CR1 loci, that directs recombinase activity to gut macrophages<sup>48</sup> and harbor 'floxed' *Il10ra* alleles<sup>49</sup> (*Cx3cr1<sup>cre</sup>:Il10ra<sup>fl/fl</sup>* mice) develop severe early onset colitis<sup>46</sup>. In IBD patients, intestinal colonic macrophages unable to sense IL10 due to an IL10Ra deficiency fail to be 'tamed'<sup>45,50</sup>. Collectively, our murine colitis model, driven by IL10ra deficient pro-inflammatory macrophages, allows us to study the initiation and progression of early onset colitis in IBD patients.

## **Il23-Il22 axis in IBD mouse models and human patients**

Il10r deficient macrophages display a pro-inflammatory expression profile, including the up-regulation of Il23<sup>46</sup>, a cytokine composed of two subunits - p19 unique to Il23 and p40, which is shared with Il12<sup>51</sup>. The role of Il23 in the pathogenesis of different colitis models has been thoroughly studied. Following *Helicobacter hepaticus* (*Hh*) infection of *Rag2*<sup>-/-</sup> mice, antibody-mediated neutralization of p19 or p40, but not p35, the second subunit of Il12, ameliorated disease<sup>52</sup>. Likewise, lymphopenic *Il23a*<sup>-/-</sup>:*Rag1*<sup>-/-</sup> or *Il12b*<sup>-/-</sup>:*Rag1*<sup>-/-</sup> mice are protected from T cell transfer-induced colitis, while p35-deficient mice exhibited colonic inflammation similar to that of wild type (WT) mice<sup>52</sup>. Moreover, also following a combination of *Hh* infection and IL10R blockade WT and *Il12a*<sup>-/-</sup> mice succumb to disease, whereas *Il12b*<sup>-/-</sup> mice are spared<sup>53</sup>. Notably, infection with *Hh* itself was shown to induce Il23 production by myeloid cells in these models<sup>52,54</sup>. As for the mechanism by which Il23 drives inflammation, involvement of Ifng-secreting Th1 cells and reduced Il17 levels were proposed, although differentiation of Th17 cells was unaltered in absence of Il23. Supporting the notion of Il23 action on T cells, adoptive transfer of Il23r-deficient naïve T cells into immuno-deficient mice causes less severe colitis than WT T cell transfer<sup>55</sup>.

A major response to Il23 exposure is the production of Il22, a cytokine generally considered anti-inflammatory in colitis context and acting on epithelial cells (EC). Il22 therapy by gene transfer was shown to ameliorate colitis through triggering EC mucus secretion<sup>56</sup>. Il22-producing neutrophils were shown to ameliorate colitis<sup>57</sup>. Likewise, Il22-deficient mice display increased gut inflammation, both in the DSS and the T-cell transfer colitis model<sup>58</sup>. Of note, in other inflammatory diseases, such as psoriasis<sup>59</sup>, Il22 was shown to play a pathogenic role. Pro-inflammatory activities of Il22 in the gut were so far however only reported for an innate-driven colitis model based on the injection of anti-CD40 antibody, which stimulates myeloid cells<sup>60</sup>. Neutralization of Il22, but not Il17, ameliorated disease in this study and Il22 was proposed to regulate neutrophil recruitment and tissue remodeling<sup>60</sup>. The importance of Il22 in gut homeostasis is further underlined by the existence of Il22 binding protein (Il22BP), a physiological factor titrating its activity<sup>61</sup>.

## Results – Part 1

### **IL10ra-deficient macrophages confer microbiota-dependent spontaneous colitis involving the IL23 / IL22 axis**

In both man and mice, intestinal macrophages require IL10 signalling to maintain gut homeostasis<sup>45,46,50,62</sup>. Accordingly, *Cx3cr1<sup>cre</sup>:Il10ra<sup>fl/fl</sup>* mice that harbour IL10ra-deficient macrophages develop spontaneous colitis manifested in IBD hallmarks, including tissue remodelling and immune cell infiltrates in the colon, but not the ileum<sup>46</sup>. Gene expression analysis by RNA-seq of sorted intestinal macrophages extracted from colonic lamina propria of 6 weeks old pre-colitic *Cx3cr1<sup>cre</sup>:Il10ra<sup>fl/fl</sup>* mice revealed a pro-inflammatory signature (**Fig2A-B**). Mutant macrophages displayed elevated expression of cytokines and chemokine genes, including *Il23*, *Il12*, *Ccl5*, genes encoding activation markers, such as *Trem1*, and inflammatory molecules, like *Nos2* and *Saa3*. In total, 310 genes were significantly down-regulated and 355 genes were significantly up-regulated in mutant cells, as compared to control macrophages (>2-fold change, adjusted p-value<0.05).

In order to unravel the initial steps of colitis development in the *Cx3cr1<sup>cre</sup>:Il10ra<sup>fl/fl</sup>* IBD model, we established a transfer approach to monitor disease progression. Bone marrow (BM) transplants of *Cx3cr1<sup>cre</sup>:Il10ra<sup>fl/fl</sup>* mice into lethally irradiated WT recipients induced spontaneous colitis evident within 6-7 weeks following engraftment. Specifically, mice that received 'colitogenic' *Cx3cr1<sup>cre</sup>:Il10ra<sup>fl/fl</sup>* BM, but not the recipients of *Cx3cr1<sup>gfp/+</sup>* control BM, displayed attenuation of weight gain and high colonoscopic scores 7 weeks post-transplant (**Fig2C**). Colitis development of IL10 deficient mice depends on the presence of microbial stimuli<sup>11</sup>. To define microbial contributions in the *Cx3cr1<sup>cre</sup>:Il10ra<sup>fl/fl</sup>* model, we treated [*Cx3cr1<sup>cre</sup>:Il10ra<sup>fl/fl</sup>* > WT] and control BM chimeras with broad-spectrum antibiotics and monitored disease development. Antibiotics-treated *Cx3cr1<sup>cre</sup>:Il10ra<sup>fl/fl</sup>* BM recipients gained weight and displayed colonoscopic scores similar to controls (**Fig2D**). Indeed, the pro-inflammatory signature of gut macrophages isolated from 6 weeks old *Cx3cr1<sup>cre</sup>:Il10ra<sup>fl/fl</sup>* mice treated 2 weeks with antibiotics was essentially abolished as established by RNAseq analysis (**Fig2E**). Though mutant cells expressed significantly lower *Il10ra* RNA, corroborating efficient Cre-mediated recombination, only 2 and 4 genes were significantly down- and up-regulated, respectively. Notably, qRT-PCR analysis confirmed that *Ccl5*, a chemokine highly expressed in IL10ra-

deficient macrophages (**Fig2A-B**), was not induced in macrophages extracted from *Cx3cr1<sup>cre</sup>:Il10ra<sup>fl/fl</sup>* mice treated with antibiotics (**Fig2F**).

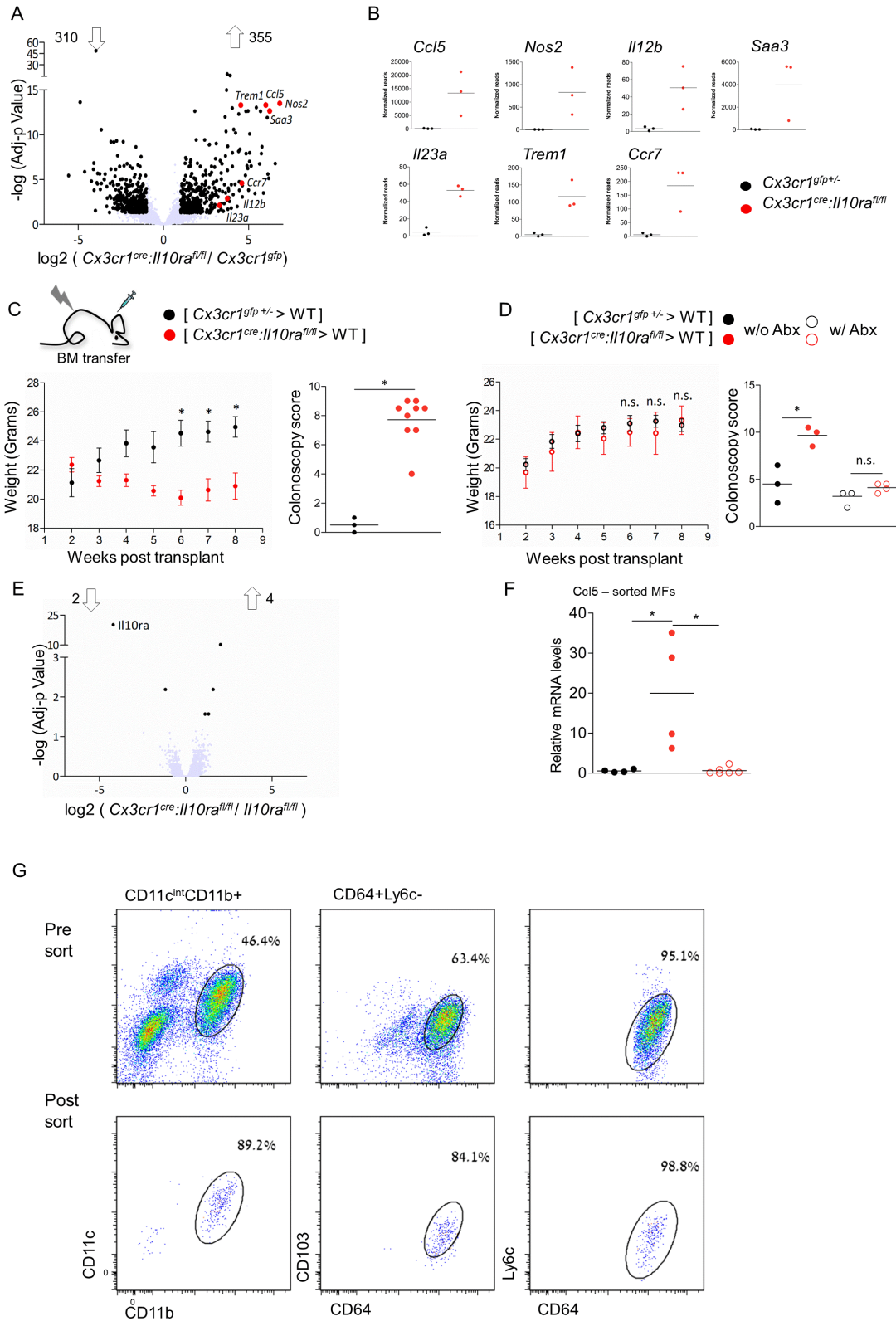
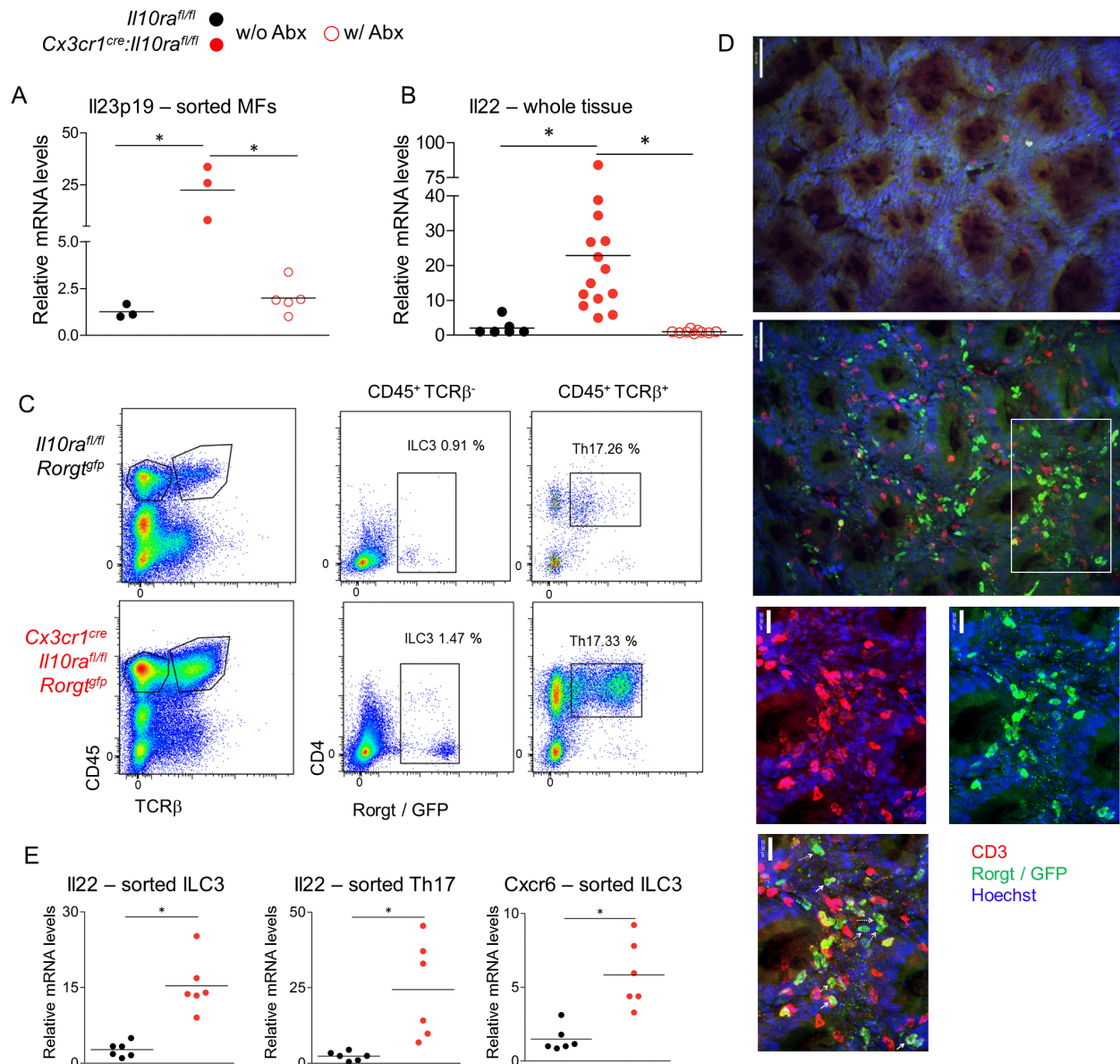


**Figure 2. Il10 receptor deficient macrophages are pro-inflammatory and cause spontaneous colitis that is prevented by antibiotics treatment**  
Figure legend on next page

IL23R was identified by GWAS as a susceptibility gene for IBD<sup>63</sup>, and Il23-deficient mice are resistant to colitis induction in different mouse models of IBD<sup>52,53</sup>. Il10ra-deficient macrophages expressed high levels of *Il23a*, as revealed by RNAseq (**Fig2A**) and confirmed by qRT-PCR conducted on sorted colonic macrophages (**Fig3A**). Antibiotics treatment abolished Il23 up-regulation. Il23 induces expression of IL22 by Th17 cells and type 3 ILC (ILC3)<sup>64,65</sup>. Indeed, Il22 levels were elevated in the tissue of mice harbouring Il10ra deficient macrophages in a microbiota-dependent manner (**Fig 3B**). Contributions of Th17 cells and ILC3 to colitis development remain controversial<sup>14</sup>. To study their role in the present colitis model, we crossed *Cx3cr1<sup>cre</sup>:Il10ra<sup>fl/fl</sup>* animals to *Rorgt<sup>gfp</sup>* reporter mice<sup>66,67</sup>, allowing identification and discrimination of ILC3 and Th17 cells by flow cytometry and histology (**Fig 3C, D**). The lamina propria of colitic *Cx3cr1<sup>cre</sup>:Il10ra<sup>fl/fl</sup>:Rorgt<sup>gfp</sup>* mice was abundantly populated with ILC3 and Th17 cells (**Fig 3D**), both of which expressed elevated *Il22* RNA levels as compared to cells isolated from *Il10ra<sup>fl/fl</sup>:Rorgt<sup>gfp</sup>* control littermates (**Fig 3E**). ILC3 extracted from colitic mice also expressed elevated levels of *Cxcr6*, a chemokine receptor critical for the localization and Il22 production in the small intestine<sup>68</sup>. Collectively, Il23-Il22 signalling axis is activated in *Cx3cr1<sup>cre</sup>:Il10ra<sup>fl/fl</sup>* mice in a microbiota-dependent manner. Pro-inflammatory intestinal macrophages that lack Il10r signalling secrete Il23, and thereby promote the accumulation and Il22 secretion of both Th17 cells and ILC3.

**Figure 2. Il10 receptor deficient macrophages are pro-inflammatory and cause spontaneous colitis that is prevented by antibiotics treatment**

(A) Volcano plot of statistical significance (-log<sub>10</sub> p-value) against log<sub>2</sub> ratio of macrophages sorted from the colonic lamina propria *cx3cr1<sup>cre</sup>il10ra<sup>fl/fl</sup>* and *cx3cr1<sup>gfp/+</sup>* mice, based on RNA-seq data. Significantly up or down regulated genes (fold change>2, adj-p value<0.05) are in black, relevant pro inflammatory up-regulated genes are highlighted in red. Data is representative of 2 independent experiment (2nd experiment is presented in figure 4a), in each experiment n>=3 for each group. (B) RNA-seq normalized read numbers for single genes of interest are plotted separately, each dot represents one mouse. (C-D) Weight and colonoscopic analysis of [*cx3cr1<sup>cre</sup>il10ra<sup>fl/fl</sup>* > WT] or [*cx3cr1<sup>gfp/+</sup>* > WT] BM chimeras, non-treated or treated with broad spectrum antibiotics. Colonoscopy was performed 7 weeks post-transplant. For non-treated mice data is representative of 3 independent experiments, n>=3 for each group. For antibiotics treated mice data are from 2 experiments. \*p<0.05. (E) Volcano plot of statistical significance (-log<sub>10</sub> p-value) against log<sub>2</sub> ratio of macrophages sorted from the colonic lamina propria of *cx3cr1<sup>cre</sup>il10ra<sup>fl/fl</sup>* and *il10ra<sup>fl/fl</sup>* co-housed littermates continuously treated with broad spectrum antibiotics given upon weaning, based on RNA-seq data. Significantly up or down regulated genes (fold change>2, adj-p value<0.05) are in black. Cre+ mice are collected from 2 independent experiments (n=2 in each), littermates are from one experiment (n=3). (F) qRT-PCR analysis of *ccl5* expression of macrophages sorted from the colonic lamina propria of indicated mice. Data is collected from 2 independent experiments, n>=3 in each. (G) Gating strategy for sorting of colonic lamina propria macrophages.



## The epithelial cell response to pro-inflammatory macrophages

The main sensors of Il22 in the colon are EC<sup>69</sup>. To determine the epithelial response of *Cx3cr1<sup>cre</sup>:Il10ra<sup>fl/fl</sup>* mice, we resorted to a reporter-based system, avoiding contaminations by immune cells, which reside in the epithelial layer. Specifically, we took advantage of *Villin<sup>cre</sup>:R26<sup>tdTomato</sup>* mice<sup>70</sup>, whose colonic and ileal EC, but not CD45<sup>+</sup> cells, express high levels of tomato reporter protein, as detected both by histology and flow cytometry (**Fig4A, B**). To induce colonic inflammation in *Villin<sup>cre</sup>:r26<sup>tdTomato</sup>* mice, we used the above BM engraftment strategy (**Fig2E**). Of note, colonic EC extracted from irradiated mice showed few differentially expressed genes as compared to EC isolated from non-irradiated animals and hence do not display persistent transcriptomic changes (**Fig4C, E**), in agreement with their reported efficiency to cope with irradiation damage<sup>71</sup>.

Colitogenic *Cx3cr1<sup>cre</sup>:Il10ra<sup>fl/fl</sup>* BM (**Fig2E**) was grafted into irradiated *Villin<sup>cre</sup>:r26<sup>tdTomato</sup>* recipients and Tomato<sup>+</sup> colonic and ileal EC were isolated from the same animal at two time points, e.g. prior to disease onset (14 days post-transplant (pt)) and upon signs of colonic inflammation (60 days pt) (**Fig5A**). RNAseq analysis revealed significant transcriptome changes of colonic EC already at day 14, and even more so at day 60 pt, with 316 and 834 differentially expressed genes, respectively (**Fig5B**). In contrast, ileal EC showed minimal changes even at day 60 pt (13 differentially expressed genes) (**Fig5B**). Differentially expressed genes at both early and late time points comprised prominent a signature of Il22-induced genes<sup>14,69</sup> and including anti-microbial peptides (AMP) and chemokines (**Fig5C**). Importantly, this 'Il22 response' was absent from the ileal EC transcriptomes (**Fig5C**). Robust AMP and chemokine up-regulation was not restricted to colitic BM chimeras, but also observed in colonic tissue of *Cx3cr1<sup>cre</sup>:il10ra<sup>fl/fl</sup>* mice, which displayed significant up-regulation of *Reg3b*, *Reg3g*, *Cxcl1* and *Cxcl5* already at 6-7 weeks of age when signs of colitis were mild, as compared to co-housed *Il10ra<sup>fl/fl</sup>* control littermates (**Fig5D**). To confirm that the source of AMPs in *Cx3cr1<sup>cre</sup>:Il10ra<sup>fl/fl</sup>* mice was epithelial cells, we sorted CD45<sup>-</sup> cells from the epithelial fraction. This population of cells will include mostly epithelial cells, but also endothelial cells, stromal cells and fibroblasts. Indeed, CD45<sup>-</sup> cells sorted from the epithelial fraction of pre-colitic *Cx3cr1<sup>cre</sup>:Il10ra<sup>fl/fl</sup>* but not *Il10ra<sup>fl/fl</sup>* mice expressed up-regulated levels of AMPs (**Fig5E**).

In conclusion, colonic EC readily respond to pro-inflammatory macrophages prior to overt signs of intestinal inflammation, including expression of Il22-induced genes.

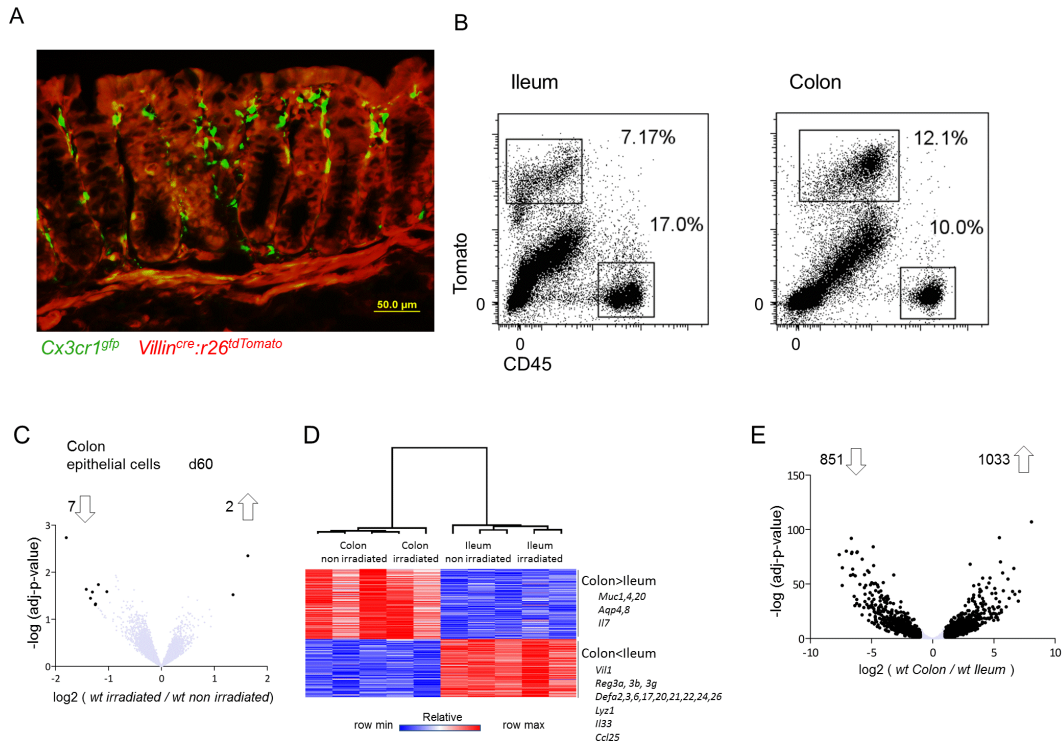


**Figure 4. Analysis of epithelial cells in *Villin<sup>cre</sup>:r26-tdTomato* mice**

(A) Representative picture of microscopic analysis of *[Cx3cr1<sup>gfp</sup> > Villin<sup>cre</sup>:r26-tdTomato]* BM chimera. (B) Representative picture of flow cytometry analysis and sorting strategy of *[Cx3cr1<sup>gfp</sup> > Villin<sup>cre</sup>:r26-tdTomato]* BM chimera. (C) Volcano plot of statistical significance ( $-\log_{10}$  p-value) against  $\log_2$  ratio between colonic epithelial cells sorted from *[Cx3cr1<sup>gfp/+</sup> > Villin<sup>cre</sup>:r26-tdTomato]* BM chimeras and *Villin<sup>cre</sup>:r26-tdTomato* mice based on RNA-seq data. Significantly up or down regulated genes (fold change > 2, adj-p value < 0.05) are in black. (D) Heat map displaying RNA-seq data of sorted colonic and ileal epithelial cells from *[Cx3cr1<sup>gfp/+</sup> > Villin<sup>cre</sup>:r26-tdTomato]* BM chimeras and *Villin<sup>cre</sup>:r26-tdTomato* mice. Presented are 1884 genes significantly differentially expressed (fold change > 2, adj-p value < 0.05) between colon and ileum. Normalized read number were log transformed and clustered by a Pearson correlation test and number of partition clusters was set to two. Samples were hierarchically clustered by a Pearson correlation test. (E) Volcano plot of statistical significance ( $-\log_{10}$  p-value) against  $\log_2$  ratio between colonic and ileal epithelial cells sorted from *Villin<sup>cre</sup>:r26-tdTomato* mice based on RNA-seq data. Significantly up or down regulated genes (fold change > 2, adj-p value < 0.05) are in black.

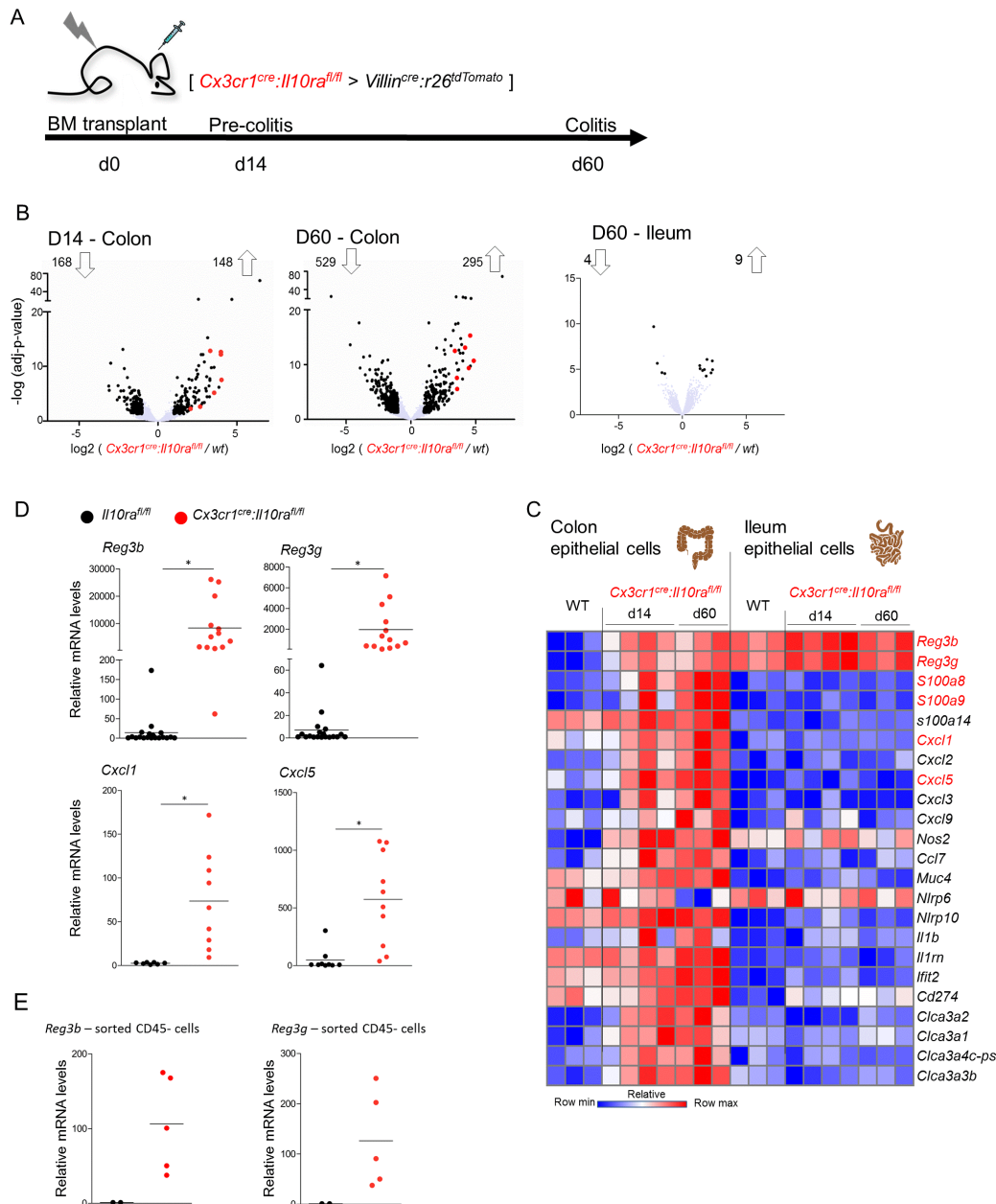


**Figure 5. The response of epithelial cells to pro-inflammatory macrophages**

(A) Description of BM chimera experiment and timeline of epithelial cell harvest. (B) Volcano plot of statistical significance ( $\log_{10}$  p-value) against  $\log_2$  ratio of epithelial cells sorted from the colon or ileum of  $[cx3cr1^{cre};il10ra^{fl/fl} > Villin^{cre};r26-tdTomato]$  BM chimeras and  $Villin^{cre};r26-tdTomato$  mice, based on RNA-seq data. Significantly up or down regulated genes (fold change  $>2$ , adj-p value  $<0.05$ ) are in black, il22 induced genes are highlighted in red. Data is from 1 experiment,  $n \geq 3$  for each group. (C) Heatmap of RNA-seq data of colonic and ileal epithelial cells extracted from the same mouse. Normalized reads number were log transformed. Presented are genes of interest, significantly upregulated in colonic but not ileal epithelial cells in response to pro-inflammatory macrophages at both disease stages (d14 and d60 post-transplant). Known il22 induced genes are in red. (D) qRT-PCR analysis of *reg3b*, *reg3g*, *cxcl1* and *cxcl5* expression in whole tissue extracts of colons of indicated mice. Data collected from 2 independent experiments,  $n \geq 3$  in each. (E) qRT-PCR analysis of *reg3b* and *reg3g* expression in sorted colonic epithelial cells (CD45- fraction) of  $Cx3cr1^{cre};Il10ra^{fl/fl}$  mice and littermate controls

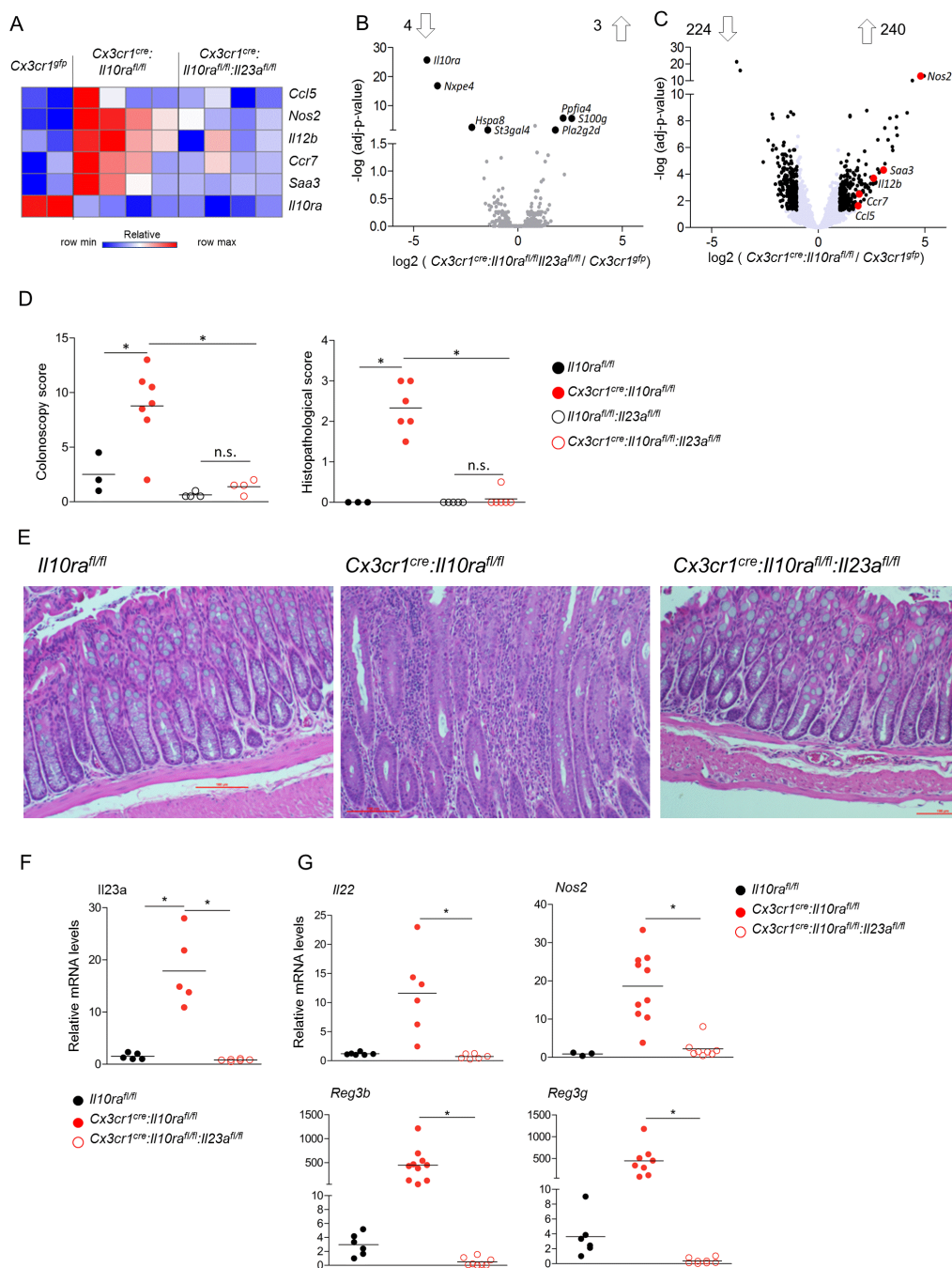


### Figure 6. II23a-deficiency prevents the colitogenic activity of II10 receptor-mutant macrophages

(A-B) Volcano plot of statistical significance (log<sub>10</sub> p-value) against log<sub>2</sub> ratio of macrophages sorted from the colonic lamina propria of *cx3cr1<sup>cre</sup>il10ra<sup>fl/fl</sup>* and *cx3cr1<sup>gfp/+</sup>* mice (A) or *cx3cr1<sup>cre</sup>il10ra<sup>fl/fl</sup>il23a<sup>fl/fl</sup>* and *cx3cr1<sup>gfp/+</sup>* mice, based on RNA-seq data. Significantly up or down regulated genes (fold change > 2, adj-p value < 0.05) are in black, relevant pro inflammatory up-regulated genes are highlighted in red. In (A) Data is representative of 2 independent experiment (second experiment is presented in figure 1a), in each experiment n >= 3 for each group. In (B) data is of one experiment, n >= 3 for each group. (C) Heatmap of RNA-seq data of colonic macrophages sorted from indicated mice. Normalized reads number were log transformed. (D) qRT-PCR analysis of *il23a* expression by sorted colonic macrophages of indicated mouse strains. Data is collected from 2 independent experiments, n >= 3 in each. (E) Colonoscopic (left) and histopathological (right) analysis of indicated mouse strains. Colonoscopy data is 1 representative experiment of 2, n >= 3 in each, histopathological analysis data is collected from 2 independent experiments, n >= 3 in each. (F) Representative images of histopathological analysis of indicated mouse strains. (G) Representative plots of flow cytometry analysis of the colonic lamina propria of indicated mouse strains. (H) qRT-PCR analysis of *il22*, *reg3b*, *reg3g* and *nos2* expression in colonic whole tissue RNA extracts of indicated mouse strains. Data collected from 2 independent experiments, n >= 3 in each.

## Mutant macrophage production of Il23 drives colitis in *Cx3cr1<sup>cre</sup>:Il10ra<sup>fl/fl</sup>* mice

Although the central role of Il23 has been established for other IBD models<sup>52,53</sup>, cellular sources of this cytokine remain controversial<sup>72-74</sup>. Moreover, in addition to Il23, colonic Il10r deficient macrophages produce other pro-inflammatory factors, including Il6, Il1, TNF and Ccl5, challenging the assumption that macrophage-derived Il23 is the sole driver of pathology. To nevertheless probe for such a scenario in the *Cx3cr1<sup>cre</sup>:Il10ra<sup>fl/fl</sup>* colitis model, we generated *Cx3cr1<sup>cre</sup>:Il10ra<sup>fl/fl</sup>:Il23a<sup>fl/fl</sup>* mice<sup>75</sup>. Strikingly, intestinal macrophages of these animals, which in addition to failing to sense Il10 are unable to produce Il23, lost their complete pro-inflammatory signature (**Fig6A,B**). Il10ra / Il23 double-deficient cells displayed only 7 differentially expressed genes (**Fig6B**), in contrast to *Cx3cr1<sup>cre</sup>:Il10ra<sup>fl/fl</sup>* macrophages isolated from littermate mice (**Fig6C**).

Mere neutralization of macrophage-derived Il23 rescued *Cx3cr1<sup>cre</sup>:Il10ra<sup>fl/fl</sup>:Il23a<sup>fl/fl</sup>* mice from colitis, as was evident from colonoscopy and histopathological analysis of co-housed age matched littermates (**Fig6D,E**). In absence of Il23 secretion by macrophages (**Fig6F**) tissue *Il22* expression returned to homeostatic levels, as did expression of *Reg3b*, *Reg3g* and *Nos2* genes (**Fig6G**). Data obtained from complementary BM chimeras corroborated the above observation (**Fig7A-B**). Collectively, these data establish that the critical Il23 source driving colitis in the *Cx3cr1<sup>cre</sup>:Il10ra<sup>fl/fl</sup>* colitis model are macrophages, i.e. the same cells that lack Il10 signalling. Moreover, our results emphasize the importance of Il23 for disease initiation and that this factor directly or indirectly induces a secondary pro-inflammatory gene signature in the macrophages.

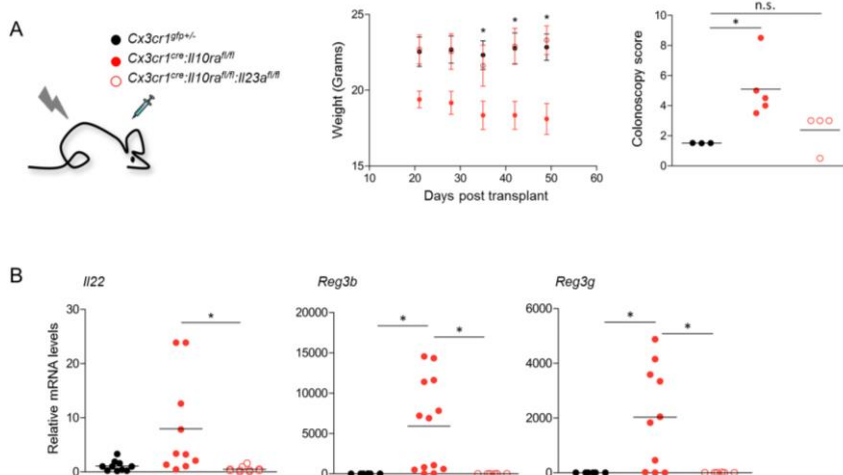


**Figure 7. Macrophage derived Il23a is critical for colitis induction in BM chimeras model** (A) Weight and colonoscopic analysis of [ *Cx3cr1<sup>cre</sup>:Il10ra<sup>fl/fl</sup>* > WT ], [ *Cx3cr1<sup>gf/p/+</sup>* > WT ] or [ *Cx3cr1<sup>cre</sup>:Il10ra<sup>fl/fl</sup>:Il23a<sup>fl/fl</sup>* > WT ] BM chimeras. Colonoscopy was performed 6 weeks post-transplant. Weight data is collected from 2 independent experiments, colonoscopy data is representative of 2 independent experiments, n>=3 in each. (B) qRT-PCR analysis of *il22*, *reg3b* and *reg3g* expression in colonic whole tissue RNA extracts of indicated BM chimeric mice. Data collected from 2 independent experiments, n>=4 in each.

### **IL22 is required for IL23 driven colitis in *Cx3cr1<sup>cre</sup>:Il10ra<sup>fl/fl</sup>* mice**

IL23 induces ILC3, Th17 cells and neutrophils to produce IL22<sup>57</sup>, which is widely considered to be beneficial<sup>56,58</sup>, but was also reported to be harmful<sup>60</sup>. Given the strong epithelial 'IL22 response' to IL10r-deficient macrophages (**Fig5C**), we next tested the impact of IL22 in the *Cx3cr1<sup>cre</sup>:Il10ra<sup>fl/fl</sup>* colitis model. Specifically, we crossed *Cx3cr1<sup>cre</sup>:Il10ra<sup>fl/fl</sup>* mice to *Il22<sup>-/-</sup>* animals<sup>58</sup>. Interestingly, the resulting *Cx3cr1<sup>cre</sup>:Il10ra<sup>fl/fl</sup>:Il22<sup>-/-</sup>* mice did not develop signs of colitis, as determined by colonoscopy (**Fig8A**) and histopathological evaluation of age matched mice (**Fig8B**). Furthermore, neutrophil recruitment to the intestinal lamina propria was strongly reduced, and neutrophil numbers returned to homeostatic levels in IL22 deficient mice (**Fig8C-D**). Levels of *Il22*, *Reg3b*, *Reg3g* and *Nos2* in the colonic tissue were reduced and similar to those of WT littermates in *Cx3cr1<sup>cre</sup>:Il10ra<sup>fl/fl</sup>:Il22<sup>-/-</sup>* mice (**Fig8E**). This established IL22 as a pro-inflammatory factor that is essential for colitis induction in the *Cx3cr1<sup>cre</sup>:Il10ra<sup>fl/fl</sup>* model.

Unexpectedly though, when we aimed to corroborate this finding in complementary BM chimeras, WT mice that received *Cx3cr1<sup>cre</sup>:Il10ra<sup>fl/fl</sup>:Il22a<sup>-/-</sup>* BM grafts succumbed to colitis like [*Cx3cr1<sup>cre</sup>:Il10ra<sup>fl/fl</sup>* > WT] BM chimeras (**Fig9A**). Indeed, when analysed by qRT-PCR, colonic tissue of all diseased BM chimeras showed elevated AMP levels, as well as *Il22* RNA, suggesting that the latter derived from radio-resistant host cells in [*Cx3cr1<sup>cre</sup>:Il10ra<sup>fl/fl</sup>:Il22<sup>-/-</sup>* > WT] chimeras (**Fig9B**). Supporting this notion, irradiated *Il22<sup>-/-</sup>* recipients that received the otherwise colitogenic *Cx3cr1<sup>cre</sup>:Il10ra<sup>fl/fl</sup>:Il22<sup>-/-</sup>* BM were protected from colitis, as compared to WT recipients (**Fig9C**). Furthermore, in the absence of IL22 from both the recipient and the graft, *Il22*, *Reg3b* and *Reg3g* expression returned to homeostatic levels (**Fig9D**). This established IL22 as a pro-inflammatory factor that is essential for colitis induction in the *Cx3cr1<sup>cre</sup>:Il10ra<sup>fl/fl</sup>* model. Further, it suggests that the source of IL22 is a radio-resistant cell in this model.

To further define the identity of radio-resistant IL22 producing cells in *Cx3cr1<sup>cre</sup>:Il10ra<sup>fl/fl</sup>* mice, we generated BM chimeras using *Rorgt<sup>gfp</sup>* mice as recipients. These mice allow us to identify and sort the radio-resistant *Rorgt<sup>+</sup>* cells, since only recipient cells are labelled by GFP. Recipient GFP<sup>+</sup> Th17 cells, but not ILC3, were abundantly found in the lamina propria of both [*Cx3cr1<sup>cre</sup>:Il10ra<sup>fl/fl</sup>* > *Rorgt<sup>gfp</sup>*] and [*Il10ra<sup>fl/fl</sup>* > *Rorgt<sup>gfp</sup>*] mice three weeks after BM transplantation (**Fig9E**). Th17 cell numbers were significantly higher in

*Cx3cr1<sup>cre</sup>:Il10ra<sup>fl/fl</sup>* BM recipients (**Fig9E**), and sorted host Th17 cells from these BM chimeras exhibited elevated levels of Il22 transcription (**Fig9F**). These data suggest that the critical cellular source of Il22 in our mouse model of colitis is Th17 cells, rather than ILC3.

Collectively, we established an important role of Il23-Il22 signaling pathway in colitis driven by pro-inflammatory macrophages. Depletion of one of these genes was sufficient to prevent colitis development in macrophage specific Il10r deficient mice (**Fig9G**).

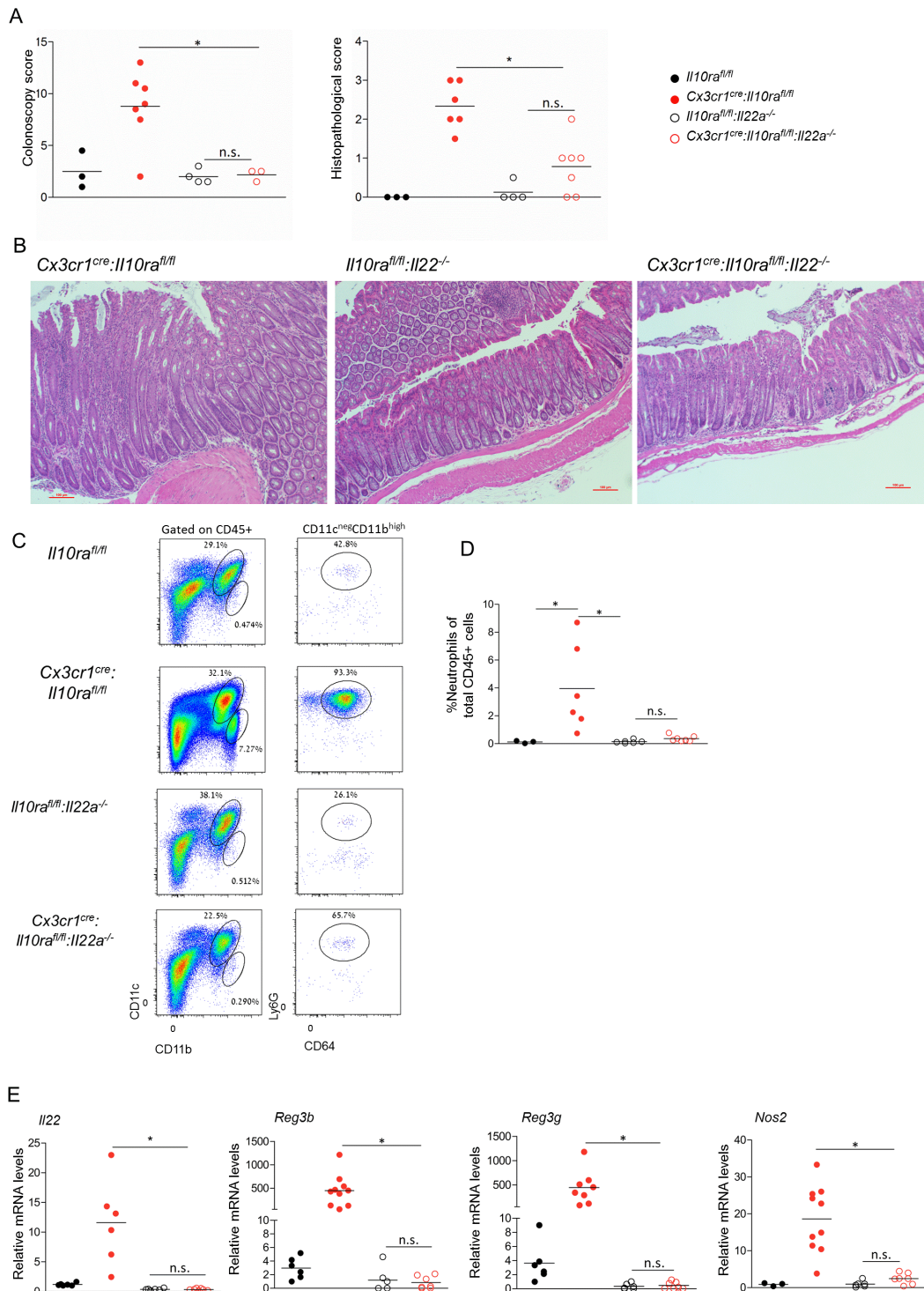


**Figure 8. II22 is critical for colitis driven by II10 receptor-deficient macrophages.**

(A) Colonoscopic (left) and histopathological (right) analysis of indicated mouse strains. Colonoscopy data is one representative experiment of 2,  $n \geq 3$  in each, histopathological analysis data is collected from 2 independent experiments,  $n \geq 3$  in each. (B) Representative images of histopathological analysis of indicated mouse strains. (C) Representative plots of flow cytometry analysis of the colonic lamina propria of indicated mouse strains. (D) Quantification of flow cytometry analysis according to gating strategy indicated in G. data is collected from 2 independent experiment,  $n \geq 3$  in each. (E) qRT-PCR analysis of *reg3b*, *reg3g*, *nos2* and *il22* expression in colonic whole tissue extracts of indicated mouse strains. Data collected from 2 independent experiments,  $n \geq 3$  in each.

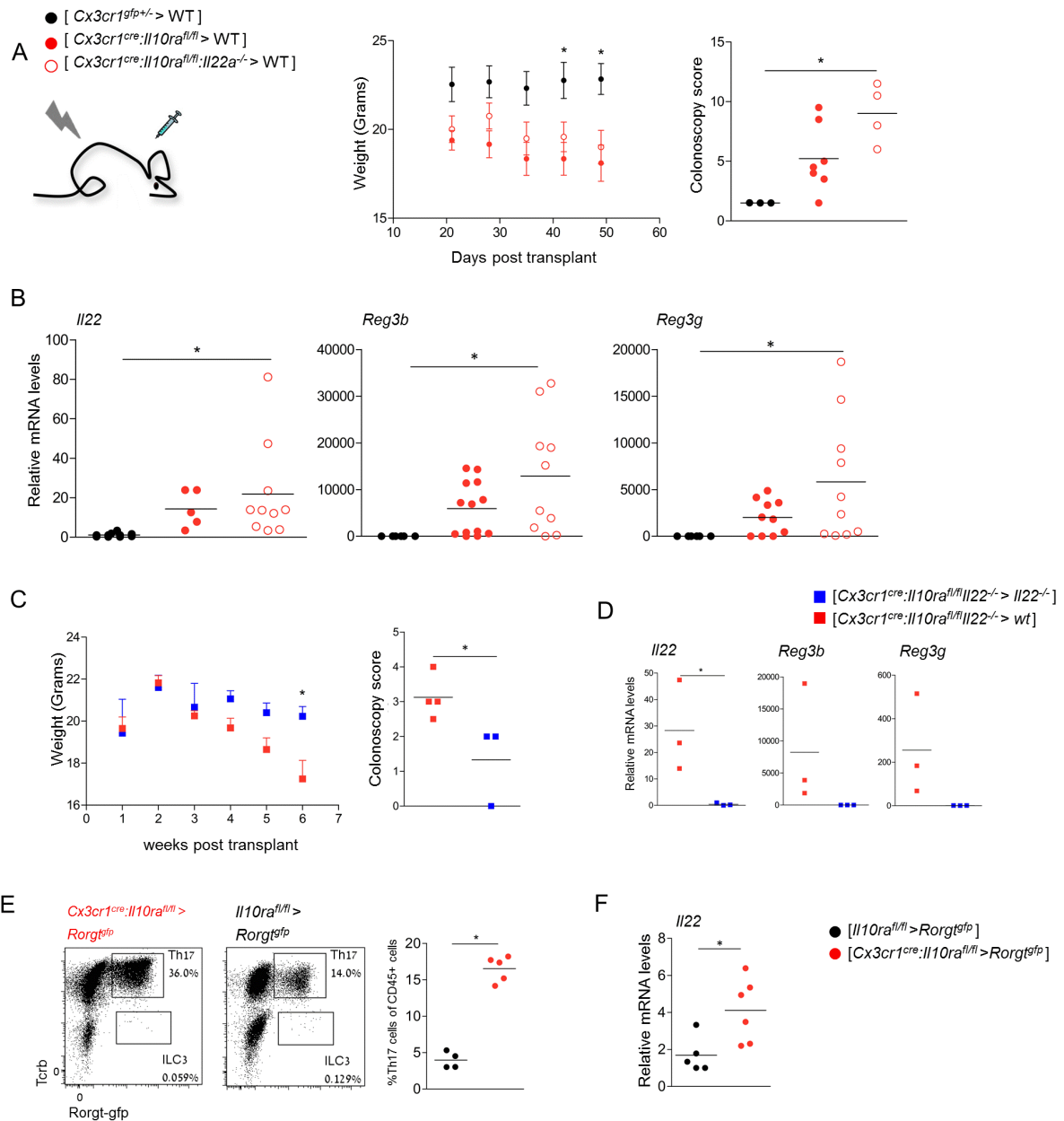


**Figure 9. Cellular source of IL22 are Th17 cells** (A) Weight and colonoscopic analysis of [ *Cx3cr1<sup>cre</sup>:Il10ra<sup>fl/fl</sup>* > WT ], [ *Cx3cr1<sup>gfp/+</sup>* > WT ] or [ *Cx3cr1<sup>cre</sup>:Il10ra<sup>fl/fl</sup>:Il22<sup>-/-</sup>* > WT ] BM chimeras. Colonoscopy was performed 6 weeks post-transplant. Weight data is collected from 2 independent experiments, colonoscopy data is representative of 2 independent experiments, n>=3 in each. (B) qRT-PCR analysis of *reg3b*, *reg3g* and *il22* expression in whole tissue extracts of colons of indicated BM chimeric mice. Data are collected from 3 independent experiments, n=3-5 in each group. (C) Weight and colonoscopic analysis of [ *Cx3cr1<sup>cre</sup>:Il10ra<sup>fl/fl</sup>:Il22<sup>-/-</sup>* > WT ], [ *Cx3cr1<sup>cre</sup>:Il10ra<sup>fl/fl</sup>:Il22<sup>-/-</sup>* > *Il22<sup>-/-</sup>* ] BM chimeras. Colonoscopy was performed 7 weeks post-transplant. Weight data are from one representative experiment of two experiments, n=3-4 in each group, colonoscopy data are from one experiment. (D) qRT-PCR analysis of *reg3b*, *reg3g* and *il22* expression in whole tissue extracts of colons of indicated BM chimeric mice. Data are from one experiment. (E) Flow cytometry analysis of the lamina propria of [ *Cx3cr1<sup>cre</sup>:Il10ra<sup>fl/fl</sup>* > *Rorgt<sup>gfp</sup>* ], [ *Il10ra<sup>fl/fl</sup>* > *Rorgt<sup>gfp</sup>* ] BM chimeras. Data are representative of two experiments, n=3-5 in each group. (F) qRT-PCR analysis of *il22* expression by sorted Th17 cells from indicated BM chimeras. Data are collected from two independent experiments, n=3-5 in each group.

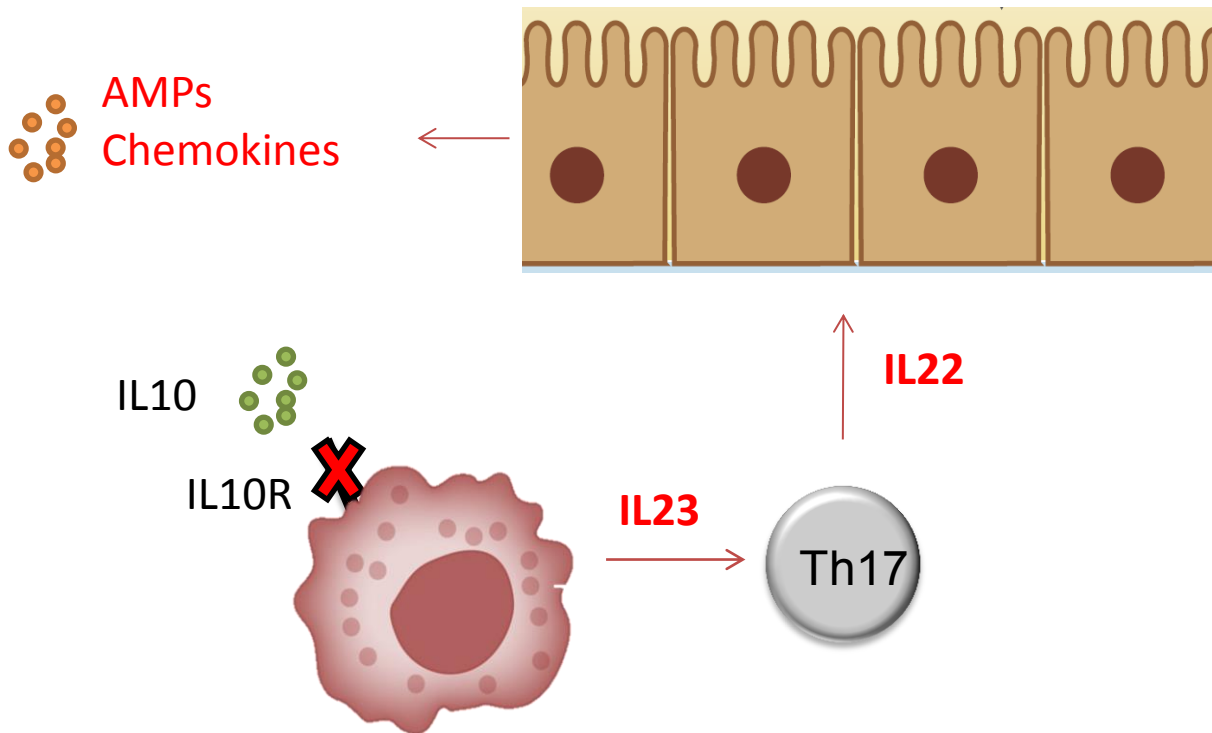


**Figure 10** - Proposed model of colitis development in *Cx3cr1<sup>cre</sup>;Il10ra<sup>fl/fl</sup>* mice

### Discussion – part 1

Here we focused on understanding the critical steps in induction and progression of pro-inflammatory macrophages driven colitis.

*Cx3cr1<sup>cre</sup>* mice allow to specifically and efficiently target colonic tissue macrophages, sparing classical DC and neutrophils<sup>48</sup>.

Using this system we had previously shown that Il10 production by colonic macrophages (*Cx3cr1cre:Il10fl/fl* mice) is not critical for maintenance of tissue homeostasis, suggesting a different source of Il10 in the tissue<sup>46</sup>. Work published by the Rudensky group suggested that T regulatory cells are the critical source for Il10<sup>47</sup>. However, we established that Il10 sensing by colonic macrophages is critical, since deletion of Il10r from colonic macrophages (*Cx3cr1<sup>cre</sup>:Il10ra<sup>fl/fl</sup>* mice) caused severe spontaneous colitis<sup>46</sup>. We further investigated colitis development in these mice.

Recently, *Il10r* deficient mice were shown to develop signs of colitis upon weaning from breast milk, meaning as early as three weeks old<sup>76</sup>. Similarly, children harboring IL10R mutated alleles develop very early onset colitis, and show signs of intestinal inflammation already during infancy<sup>45</sup>. Although in our mouse model the *Il10r* deficiency is restricted to macrophages, *Cx3cr1<sup>cre</sup>:Il10ra<sup>fl/fl</sup>* mice develop colitis

spontaneously and very early on. At 6-7 weeks of age we already witness vast changes in the transcriptional profile of intestinal macrophages harvested from *Cx3cr1<sup>cre</sup>:Il10rd<sup>fl/fl</sup>* mice. Thus, we wished to establish a system which will allow us to follow colitis development in a gradual manner. We found that engraftment of *Cx3cr1<sup>cre</sup>:Il10rd<sup>fl/fl</sup>* bone marrow into lethally irradiated mice resulted in gradual development of spontaneous colitis, although the recipient animals were adult healthy mice. Establishing this transfer system allowed us to follow the disease progression in these mice. Second, we discovered that colitis development is dependent on microbiome load, since antibiotics treatment abolished colitis signs and rescued the mice, both in the bone marrow chimeras model, and in *Cx3cr1<sup>cre</sup>:Il10rd<sup>fl/fl</sup>* mice. The importance of microbiome sensing by macrophages in *Il10ko* mice has been shown before, using both *Cd11c<sup>cre</sup>:MyD88<sup>fl/fl</sup>* and *Lysm<sup>cre</sup>:MyD88<sup>fl/fl</sup>* mice on the *Il10ko* background<sup>11</sup>. MyD88 is a signaling component of the TLR4 pathway. Mice that lacked TLR4 signaling in the mononuclear phagocytes compartment were rescued from colitis, meaning that sensing of the microbiome by mononuclear phagocytes is critical for colitis development. This suggests that mononuclear phagocytes and specifically macrophages are drivers of colitis in mice that lack Il10. Moreover, it emphasizes the important role of TLR signaling in *il10ko* mice, specifically in mononuclear phagocytes. We corroborate this finding by using broad spectrum antibiotics which lowers the microbial load in the gut. Interestingly, treatment of mice for 2 weeks, between the ages 4 and 6 weeks, was enough to prevent the pro-inflammatory effect of il10r deficient macrophages.

The importance of Il23 in colonic inflammation has been emphasized in several studies over the years, and we found that Il23 is secreted by Il10r deficient macrophages. This suggests that Il10 signaling is critical for suppressing Il23 transcription by colonic macrophages. One possible mechanism which could explain Il23 suppression by Il10 is via Tristetraprolin (Ttp). Ttp is an mRNA binding protein, containing zinc-finger domains through which it binds to Adenine-Uridine rich elements (ARE) in the 3'UTR of its target genes<sup>77</sup>. Binding of Ttp to a target mRNA causes de-adenylation and mRNA decay, thus controlling the translation of its target genes<sup>77</sup>. Emphasizing the importance of Ttp in maintaining homeostasis is the severe inflammatory phenotype of *Ttp<sup>-/-</sup>* mice, displaying a multi-organ auto inflammatory phenotype as early as one week after birth, including alopecia, dermatitis, arthritis and cachexia<sup>78</sup>. Ttp controls a wide variety of targets, including the cytokines TNF $\alpha$  and

GM-CSF<sup>77</sup>. Recently, Ttp was shown to control Il23p19 but not Il12p40 mRNA stability<sup>79</sup>. Interestingly, abolishing Il23 in Ttp deficient mice, reverts the phenotype and recues the mice<sup>79</sup>, suggesting that control of Il23 by Ttp is a critical mechanism in homeostasis maintenance, and further emphasizing the pro-inflammatory capacity of Il23. In another study it has been shown that Il10 signaling induces Ttp expression<sup>80</sup>. Combining the finding of these studies together suggests a possible mechanism for the control of Il23 expression by Il10 signaling, mediated by Ttp. Namely, Il10 sensing by macrophages induces Ttp expression, which in turn binds to Il23 mRNA, causing its degradation. This hypothesis should be further examined experimentally.

Furthermore, we found that the colonic environment, and specifically Th17 cells and ILC3 respond to increased Il23 levels by secreting Il22. Using our BM chimeras model we were able to establish that Th17 cells are the critical source of Il22 in our model. Finally, Il23 secretion by macrophages, as well as Il22 secreted in response, were dependent on the microbiome, since antibiotics treatment prevented their up-regulation. Epithelial cells are the main sensors of Il22, since they express the specific chain of Il22 receptor (Il22ra)<sup>69</sup>. Indeed, we observed a significant response of epithelial cells to Il22, present already in early stages of colonic inflammation. Specifically, anti-microbial genes including *Reg3b*, *Reg3g*, *S100a8* and *S100a9* were upregulated in epithelial cells triggered by Il22. Further, the chemokines *Cxcl1* and *Cxcl5* were upregulated by epithelial cells in response to Il22. These chemokines are sensed by Cxcr2, a chemokine receptor expressed by neutrophils and essential for neutrophil trafficking from the bone marrow<sup>81,82</sup>. Indeed, we detected neutrophil infiltration into the colonic tissue of *Cx3cr1<sup>cre</sup>:Il10ra<sup>fl/fl</sup>* mice, which was Il22 dependent.

We observed Il23 and Il22 elevation in the colonic tissue in early stages of the inflammatory process, but we were interested to examine whether this elevation was a result of the inflammation, or alternatively the driver of the inflammatory process. To answer this question we crossed *Cx3cr1<sup>cre</sup>:Il10ra<sup>fl/fl</sup>* mice to either *Il23a<sup>fl/fl</sup>* mice or *Il22ko* mice. Essentially, we created two new strains of mice:

- (1) *Cx3cr1<sup>cre</sup>:Il10ra<sup>fl/fl</sup>:Il23a<sup>fl/fl</sup>* mice – in these mice intestinal macrophages lack both Il10r signalling and Il23p19 production.
- (2) *Cx3cr1<sup>cre</sup>:Il10ra<sup>fl/fl</sup>:Il22ko* mice – in these mice in addition to Il10r signalling lacking from intestinal macrophages, Il22 is generally ablated from all cells.

Interestingly, both these ablations resulted in rescue of colitis. In the case of Il23, we specifically ablated it from the same cells which are ablated for Il10r signaling in our system. In this setting, the pro-inflammatory macrophages are capable of producing any cytokine, chemokine or other pro-inflammatory agent other than Il23.

Importantly, other cells of the colonic tissue which are not targeted by the Cx3cr1<sup>cre</sup> system, such as neutrophils, CD103+CD11b- DCs (also referred to as cDC1), T and B cells retain their WT genotype<sup>46,72</sup>. This emphasized the critical role of Il23 in colitis development, but more importantly the critical cellular source, which are intestinal macrophages. Previous reports used the CD11c-Cre system in order to find the cellular source of Il23, and indeed the cells targeted by the Cre recombinase in this model were found important<sup>54</sup>. However, the CD11c-Cre system is broader than Cx3cr1<sup>cre</sup>, since besides macrophages it targets all DCs and some T cells<sup>83,84</sup>.

Usually, Il22 is considered to be an anti-inflammatory cytokine in the gut context. Il22 belongs to the Il10 family of cytokines, which are generally anti-inflammatory. Il22 deficient mice display worse signs of colitis in the DSS colitis model, as well as in the T cell transfer model<sup>58</sup>. It has been shown that Il23 induces Il22 secretion, but since Il23 also induces Il17 secretion, the role of Il22 as a pro-inflammatory agent was mostly ignored. Our findings suggest that in a chronic model of colitis, driven by Il10r deficient macrophages, Il22 plays a critical pro-inflammatory role. In the absence of Il22 signs of colitis are abolished and mice are rescued from colitis.

Furthermore, using the bone marrow transfer system we found that the critical cellular source of Il22 are radio-resistant cells, and this finding allowed us to pin-point the critical cell type secreting Il22 in our model. In contrast to previous reports<sup>85</sup>, Th17 cells and not ILC3 were the radio-resistant critical source of Il22.

The pro-inflammatory role of Il22 has been identified in skin inflammation diseases such as acanthosis and psoriasis<sup>64,86</sup>. The suggested effect of Il22 in these models is induction of keratinocyte hyperplasia. In mouse models of skin inflammatory diseases blockade of either Il23 or Il22 were sufficient to prevent disease progression. In models of colonic inflammation most reports suggest Il22 as an anti-inflammatory agent, although one group found that in the anti-CD40 induced colitis it can act as a pro-inflammatory cytokine<sup>60</sup>. They suggest that the effect of Il22 on gut epithelial cells is by induction of neutrophil recruiting chemokines including Cxcl5 and Cxcl1. As mentioned, we also witness up-regulation of these chemokines by epithelial cells in our mouse model, and Il22 dependent neutrophil recruitment to the tissue. Finally,

in a *Salmonella* infection model, it has been shown that during infection there is a significant up-regulation of IL22 in the tissue, which is critical for *Salmonella* colonization. In this study it was suggested that IL22 induces anti-microbial expression profile of epithelial cells, exploited by *Salmonella* to compete with the microbiome and colonize the gut<sup>87</sup>.

The importance of IL23 in human IBD has been recently emphasized by the clinical success of *Ustekinumab*, a monoclonal antibody that specifically blocks p40, the shared subunit of IL23 and IL12. *Ustekinumab* was originally approved by the FDA for treatment of psoriasis patients in 2009, and the approval was in 2016 extended to treatment of Crohn's disease patients that failed to respond to corticosteroids or TNF blockers<sup>88,89</sup>. The advantage of *Ustekinumab* is that it does not increase the risk for infection or cancer, as opposed to the widely used TNF or integrin inhibitors<sup>88</sup>. In contrast, the role of IL22 in IBD progression remains controversial<sup>90</sup>. Although high IL22 levels were found in the mucosa of Crohn's disease and Ulcerative Colitis patients and correlated with disease severity<sup>91,92</sup>, it is still described as a beneficial agent in many reports and reviews<sup>93-97</sup>, and some even suggest IL22 delivery as a therapeutic approach for IBD<sup>59</sup>.

Our data suggest that both IL23 and IL22 are pro-inflammatory agents in colitis induced by pro inflammatory macrophages. A possible mechanism for IL22 driven inflammation is the induction of neutrophil recruiting chemokines Cxcl1 and Cxcl5, which are expressed by epithelial cells in response to IL22<sup>98-101</sup>. Neutrophil recruitment to the tissue is not exclusive for our colitis model but also occurs in anti-CD40 colitis<sup>60</sup> and DSS colitis<sup>6</sup>. This hypothesis requires further investigation, which can be performed using the mouse models and systems described in this thesis.

Table 1 – Mouse strains used in part1

Strain name	Ablated genes		Littermates / controls	Experiment
	Gene name	Cell population targeted		
<i>Cx3cr1<sup>cre</sup>:Il10ra<sup>fl/fl</sup></i>	<i>Il10ra</i>	Macrophages	<i>Il10ra<sup>fl/fl</sup></i> , <i>Cx3cr1<sup>sgfp/+</sup></i>	Colitis, BM chimeras
<i>Cx3cr1<sup>cre</sup>:Il10ra<sup>fl/fl</sup>:Il23a<sup>fl/fl</sup></i>	<i>Il10ra, Il23a</i>	Macrophages	<i>il10ra<sup>fl/fl</sup>:il23a<sup>fl/fl</sup></i>	
<i>Cx3cr1<sup>cre</sup>:Il10ra<sup>fl/fl</sup>:Il22<sup>-/-</sup></i>	<i>Il10ra</i> <i>Il22</i>	Macrophages All cells	<i>Il10ra<sup>fl/fl</sup>:Il22<sup>-/-</sup></i>	
<i>Villin<sup>cre</sup>R26-tdTomato</i>	None	-	-	Epithelial cell sorting
<i>Cx3cr1<sup>sgfp/+</sup></i>	None	-	-	WT mice

## Part 2 - Studying macrophage differentiation using a monocyte transfer model

### Introduction – Part 2

Intestinal macrophages are distinct from resident macrophages of other tissues like the brain or the liver<sup>102</sup>. The dynamic environment characterized by constant exposure to food antigens and the microbiota, forces intestinal macrophages to adapt and constantly renew from blood monocytes, generated in the BM<sup>20</sup>. Upon entry into the healthy intestinal tissue, monocytes differentiate into resident macrophages, acquiring an anti-inflammatory signature, which is important to maintain homeostasis in the tissue<sup>6</sup>. In our laboratory, we have developed a system to study this differentiation process. Specifically, we use mice expressing diphtheria toxin (DTx) receptor (DTR) under a specific promoter. We use both CD11c-DTR mice<sup>103,104</sup>, which allow a broad depletion of macrophages and DC, and *Cx3cr1<sup>DTR</sup>* mice that allow more specific depletion of macrophages<sup>105</sup>. Upon injection of DTx to either CD11c-DTR or *Cx3cr1<sup>DTR</sup>* recipients, the relevant cells expressing DTR will be depleted. Importantly, CD11c-DTR mice harbor a transgene, meaning that the *Dtr* gene is driven by an artificial promoter, which includes elements from the *Cd11c* gene promoter. *Cx3cr1<sup>DTR</sup>* mice in contrast harbor a *Dtr* gene driven by the endogenous *Cx3cr1* promoter. Transfer of a pure population of monocytes, isolated from BM, allows to reconstitute the population of intestinal macrophages in a synchronized way<sup>20</sup>. An interesting feature of the monocyte transfer protocol is that during the migration and differentiation of transferred monocytes in the intestinal tissue, the cells

clonally expand, creating islets of macrophages arising from the same precursor<sup>20</sup>. This phenomenon is readily observed upon transfer of a mixed population of monocytes – expressing either GFP or RFP. Combining our model of pro-inflammatory macrophages and the monocyte transfer system, we planned to dissect the steps leading to the misguided education of Il10r deficient macrophages in the tissue context.

## Results – Part 2

In order to allow efficient seeding of the tissue with transferred monocytes, we take advantage of two depleting systems available to us: CD11c-DTR and *Cx3cr1*<sup>DTR</sup> mice. To achieve sufficient numbers of differentiated macrophages in the tissue and to allow the cells to fully differentiate, we harvest the cells two weeks after the monocyte transfer. During these two weeks, depletion of endogenous cells is maintained by injection of DTx to the recipient mice every other day. Repeated DTx injection to CD11c-DTR mice results in death of the mice within a week, thus we use BM chimeras of either [CD11c-DTR >WT] or [*Cx3cr1*<sup>DTR</sup> >WT] for all our experiments. Depletion of macrophages in the *Cx3cr1*<sup>DTR</sup> system is less efficient than that in the CD11c-DTR system (**Fig11A-B**); however it is more specific, largely sparing DC. Two weeks following 50%-50% mix transfer of *Cx3cr1*<sup>gfp</sup> (WT) and *Cx3cr1*<sup>cre</sup>:*Il10ra*<sup>fl/fl</sup>:*R26Rfp*<sup>fl/fl</sup> monocytes, the small and large intestinal tissue was found seeded with colonies of GFP+ and RFP+ cells (**Fig11D**). The ratio between WT and IL10R KO macrophages in the tissue was 1, indicating that Il10r deficient macrophages are able to proliferate and differentiate similar to WT cells (**Fig11E**).

To our surprise however, unlike in the BM chimeras (**Fig 2**), Il10r deficient macrophages in the monocyte transfer set-up, failed to become pro-inflammatory. RNAseq analysis of WT and Il10r deficient macrophages harvested from monocyte transferred mice revealed that the WT and KO cells were very similar in their transcription pattern. Only 7 genes were differentially expressed, while 665 genes were differentially expressed between macrophages harvested from *Cx3cr1*<sup>gfp</sup> and *Cx3cr1*<sup>cre</sup>:*Il10ra*<sup>fl/fl</sup> mice (**Fig12A-D**). Upon mixed transfer of WT and Il10R KO cells, the same phenomenon was observed, and only 4 genes were differentially expressed. Importantly, one of the strongly down regulated genes was *Il10ra*, meaning that the Cre-recombination occurred effectively, as expected. Since we had established the

importance of Il23-Il22 pathway in our model, we wished to determine the epithelial response to Il10r deficient macrophage transfer. No upregulation of anti-microbial peptides was detected by qRT-PCR of RNA extracted from colonic whole tissue transferred with only Il10r deficient macrophages or a mix of WT and Il10r KO macrophages (**Fig13A**).

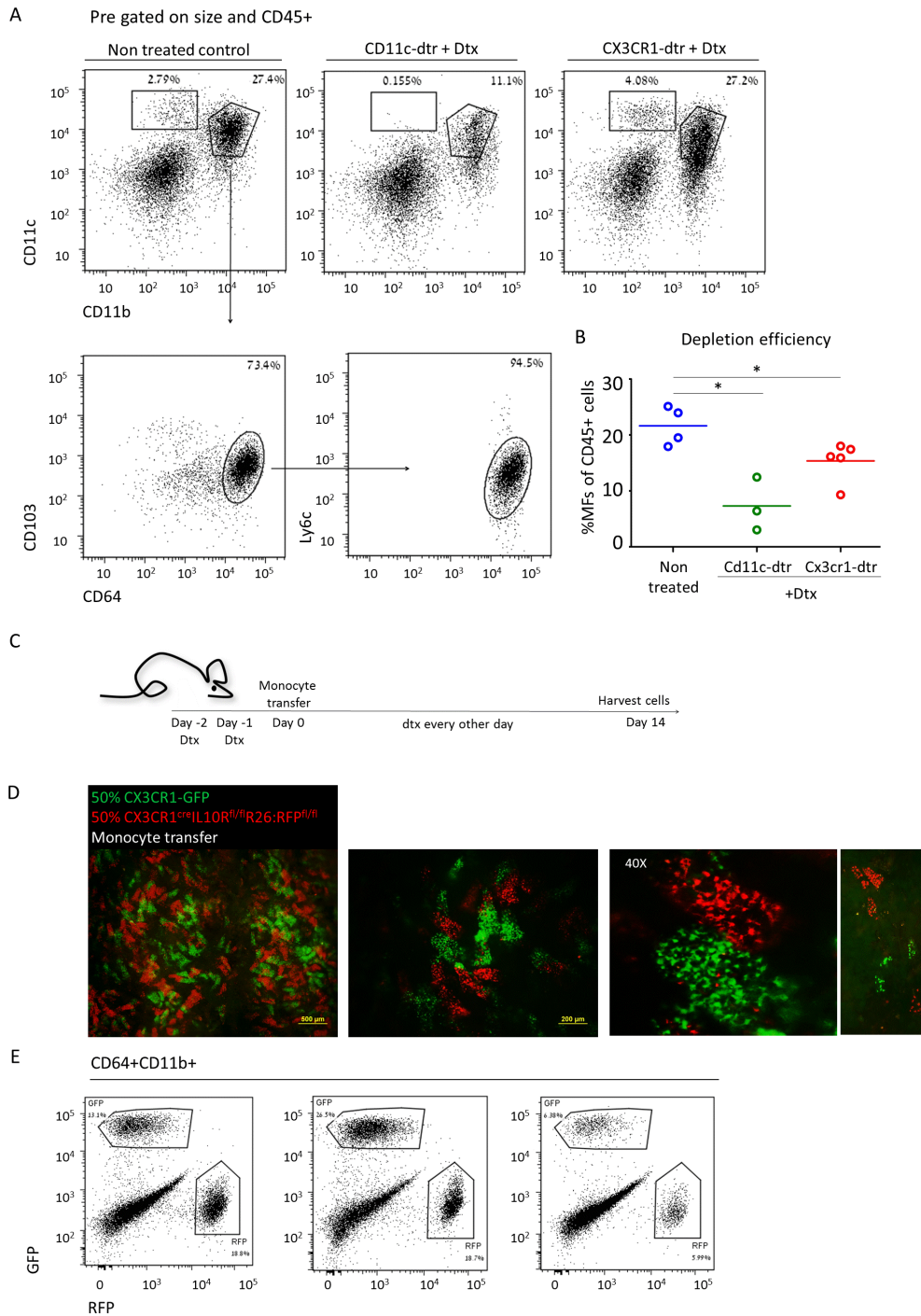


**Figure 11. Establishment of monocyte transfer system**

(A) FACS analysis of Lamina propria of the large intestine of CD11c-dtr and Cx3cr1-dtr BM chimeras following treatment with dtx (B) Quantification of macrophage depletion in Cd11c-dtr and Cx3cr1-dtr systems (C) Monocyte transfer experimental design (D) Live tissue imaging of small and large intestinal tissue and (E) Facs analysis and gating strategy of colonic tissue of Cd11c-dtr mouse 14 days post transfer with a 50%-50% mixture of Cx3cr1-gfp and Cx3cr1<sup>cre:il10ra<sup>fl/fl</sup>r26Rfp monocytes (\*p<0.05, students T-test)

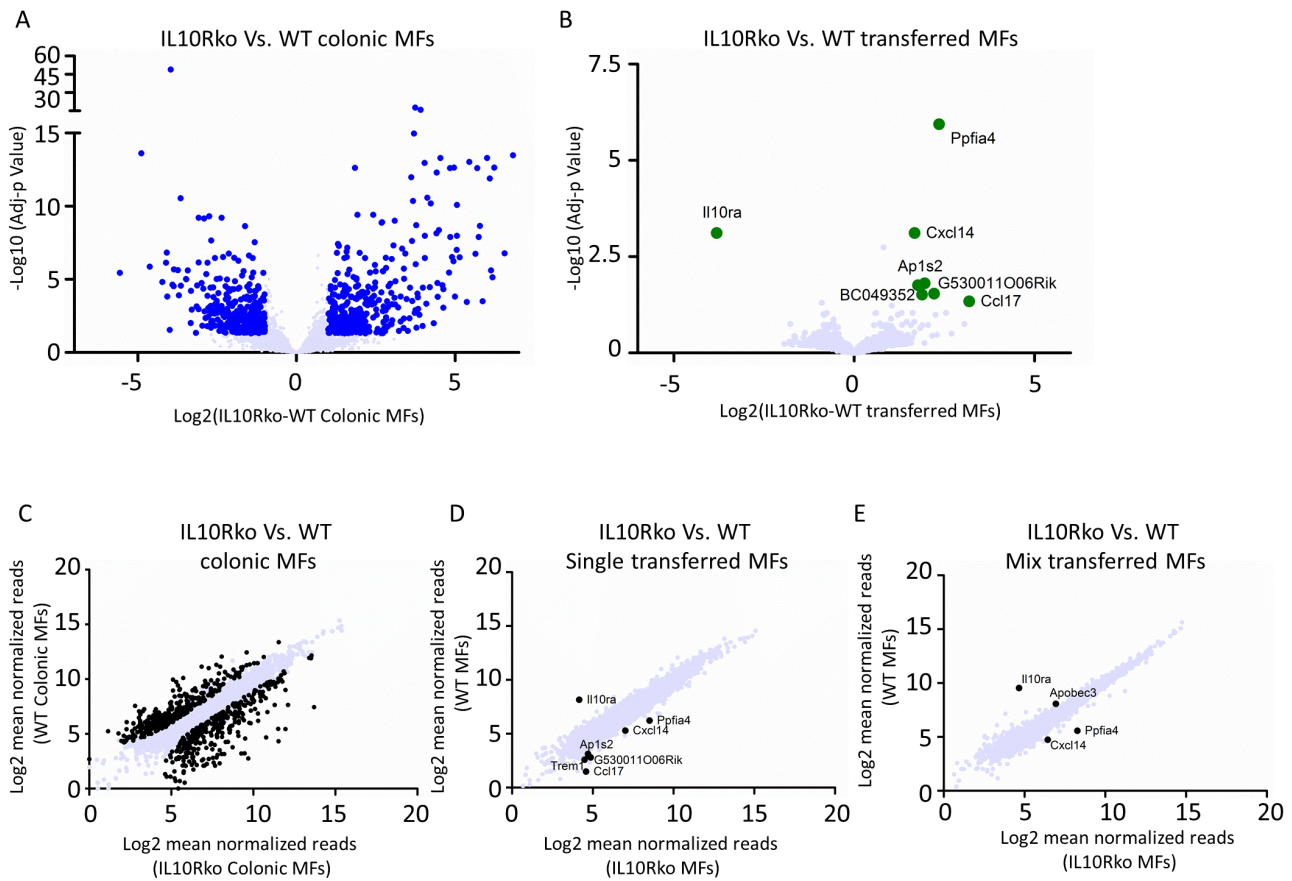


**Figure 12. IL10 Receptor deficient transferred macrophages fail to become pro-inflammatory** (A-B) Volcano plot of RNA-seq data of il10rko vs WT colonic macrophages (A) and il10rko and WT single transferred macrophages (B) (C-E) correlation analysis of RNA-seq data of (C) il10rko vs WT colonic macrophages (D) il10rko vs WT single transferred macrophages (E) il10rko vs WT mix transferred macrophages. Significantly differentially expressed genes ( $>2$  fold change,  $\text{Adj-p value} < 0.05$ ) are in bold. All transfers performed in *Cd11c-dtr* depletion system.

The *CD11c-DTR* system depletes not only macrophages, but also DC, certain mature B cells and some T cells<sup>106</sup> (**Fig11A**). We considered the possibility that the broad depletion of cells might alter the environment, in which the cells differentiate, and might prevent them from becoming pro-inflammatory. Hence, we decided to use the more specific *Cx3cr1<sup>DTR</sup>* depletion model, which allows specific depletion of cells that express *Cx3cr1*; in the gut these are mainly macrophages<sup>72</sup>. qRT-PCR analysis of the whole tissue of *Cx3cr1<sup>DTR</sup>* mice transferred with either only *Il10r* KO or a mixture of WT and KO monocytes did not cause an up-regulation of anti-microbial peptides (**Fig13B**). Next, we wanted to determine whether the time frame of 14 days is enough for the cells to acquire a pro-inflammatory signature. As mentioned, in BM chimeras, 14 days post-transplant of *Cx3cr1<sup>cre</sup>:Il10ra<sup>fl/fl</sup>* BM epithelial cells respond by up-

regulation of Il22 induced genes, among them *Reg3b* and *Reg3g* (**Fig5C**). We sought to repeat this finding, using the same donor at the same time to create BM chimeras and transferring whole BM (which includes monocytes) to *Cx3cr1<sup>DTR</sup>* mice. On the same day, the donor mice were sacrificed and the BM was split to whole-BM transplant to WT irradiated mice, and whole BM transfer to *Cx3cr1<sup>DTR</sup>* recipients. Importantly, we usually FACS or MACS-sorted monocytes, but in this case we used whole BM, which includes monocytes but also other myeloid precursors. Two weeks after transfer of cells the mice were sacrificed, and intestinal macrophages were sorted from both types of transfers: whole BM transfer to WT irradiated mice, and whole BM transfer to *Cx3cr1<sup>DTR</sup>* recipients. qRT-PCR of RNA extracted from colonic tissue revealed up-regulation of AMPs in BM chimeras, comparable to *Cx3cr1<sup>cre</sup>:Il10ra<sup>fl/fl</sup>* mice (**Fig13E**). However, BM transfer to *Cx3cr1<sup>DTR</sup>* recipients did not induce up regulation of AMPs in the whole tissue (**Fig13E**). Moreover, qRT-PCR of RNA extracted from sorted macrophages indicated that macrophages from *Cx3cr1<sup>cre</sup>:Il10ra<sup>fl/fl</sup>* BM chimeras harvested two weeks after transfer expressed high levels of Il23p19, similar to macrophages harvested from *Cx3cr1<sup>cre</sup>:Il10ra<sup>fl/fl</sup>* mice. However, macrophages isolated from *Cx3cr1<sup>DTR</sup>* recipients engrafted with *Cx3cr1<sup>cre</sup>:Il10ra<sup>fl/fl</sup>* BM exhibited very low expression of Il23p19, similar to WT mice (**Fig13F**). Additionally, we examined whether the DTx administration interferes with the pro-inflammatory phenotype of the cells, and left three transferred mice without toxin injection. The efficiency of the transfer was strongly reduced, as fewer cells were observed in the tissue two weeks following transfer (**Fig13C-D**). By qRT-PCR analysis of whole tissue RNA we did not detect an up regulation of AMPs, and qRT-PCR of RNA extracted from sorted macrophages indicated low levels of Il23p19 (**Fig13E-F**).

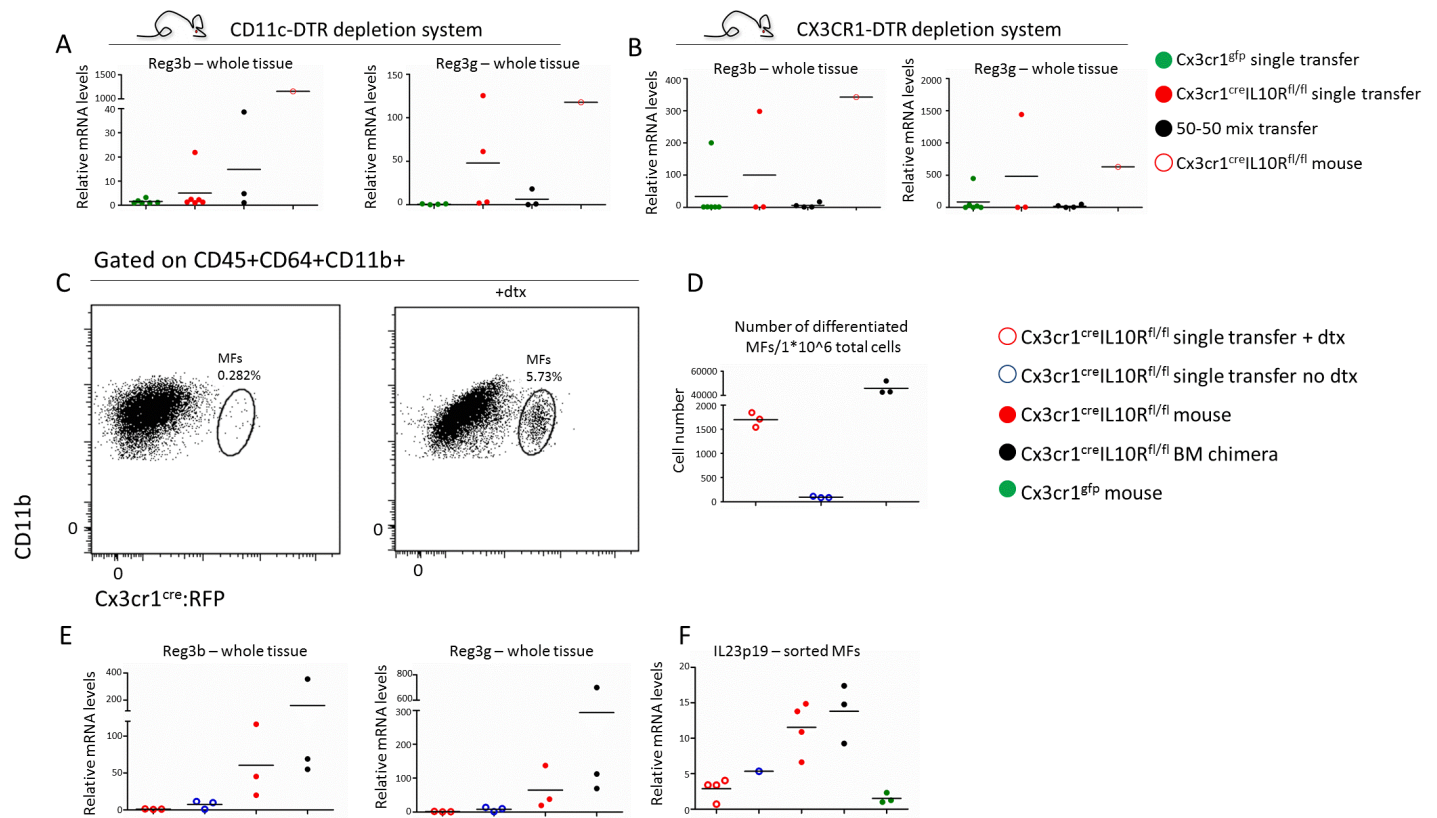


### Figure 13. Lack of response of the tissue to Il10 Receptor deficient transferred macrophages

(A-B) qRT-PCR of whole tissue RNA extracted from the indicated mice 14 days post monocyte transfer to (A) Cd11c-dtr and (B) Cx3cr1-dtr BM chimeras (C) Gating strategy of transferred macrophages and efficiency of transfer to Cx3cr1-dtr BM chimeras with and without toxin treatment (D) Quantification of macrophage numbers in transferred tissue comparing whole BM transfer to Cx3cr1-dtr BM chimeras with and without toxin treatment, and BM transfer to WT lethally irradiated mice 14 days post transfer (E) qRT-PCR of whole tissue RNA extracted from indicated mice 14 days post transfer (F) qRT-PCR of RNA extracted from macrophages sorted from the colonic lamina propria of indicated mice

Further, we explored another difference between BM chimeras and *Cx3cr1*<sup>DTR</sup> transferred mice, which is the irradiation procedure. BM chimeras are lethally irradiated 18-24 hours prior to cell transfer. Irradiation causes temporary breakage of the epithelial barrier, and increased permeability of the gut<sup>71</sup> (Fig14A). We hypothesized that sub-lethal irradiation prior to monocyte transfer could create a stimuli which is needed for development of a pro-inflammatory phenotype of Il10r-deficient cells. First, irradiation itself did not harm the efficiency of the transfer (Fig14C,E). However, cells harvested from mice irradiated prior to monocyte transfer were similar to WT in their Il23p19 expression levels (Fig14D). Additionally, *Reg3g* was not up regulated in the whole tissue of irradiated compared to non-treated mice, neither in mice transferred with WT cells nor in mice transferred with Il10r deficient monocytes.

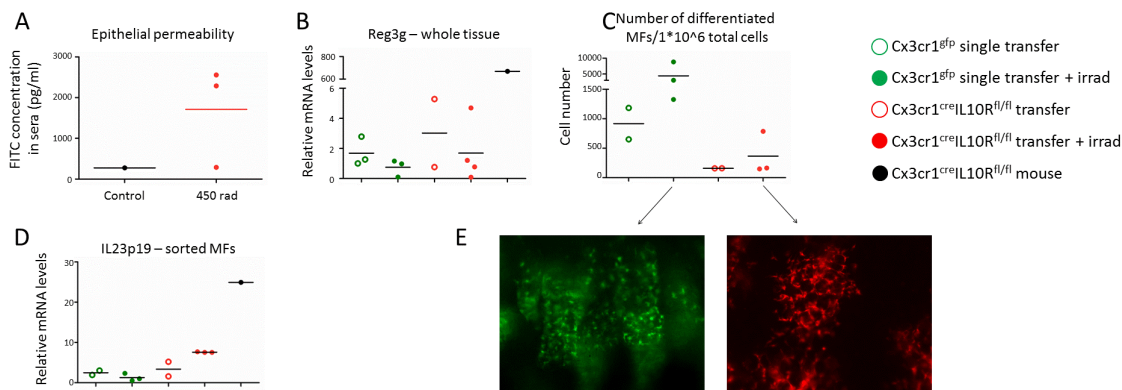


**Figure 14. Failure to induce pro-inflammatory response of transferred II10 Receptor deficient macrophages by inducing challenge**

(A) FITC concentration in the sera following gavage of 5kDa dextran as an indication for epithelial integrity (B) qRT-PCR of whole tissue RNA extracted from the indicated mice 14 days post monocyte transfer to Cx3cr1-dtr BM chimeras (C) Quantification of macrophage numbers extracted from transferred tissue (D) qRT-PCR of RNA extracted from macrophages sorted from the colonic lamina propria of indicated mice (E) Live tissue imaging of small intestine of monocyte transferred mice

Finally, we hypothesized that Tregs could inhibit the pro-inflammatory phenotype of Il10r deficient macrophages by Il10 independent mechanisms. Thus, we decided to deplete CD4 T cells with a widely used CD4 depleting antibody<sup>107</sup>. Mesenteric lymph node (mln) analysis following two i.v. injections of anti-CD4 antibody showed a significant reduction in numbers of CD4 but not CD8 T cells (Fig15A-B). CD4 depletion following monocyte transfer did not influence the efficiency of the transfer (Fig15C-E), although we witnessed some cases in both depleted and control mice, where one type of macrophages, either WT or Il10r deficient did not survive and differentiate in the tissue (Fig15D). This phenomenon requires further investigation, as it was not consistent and in some of the mice the ratio between WT and KO cells was approximately one. Lastly, qRT-PCR analysis of RNA extracted from sorted MFs of monocyte transferred mice indicated no difference in Il23 levels between WT and KO cells, neither in the control group nor in the CD4 depleted mice (Fig15F).

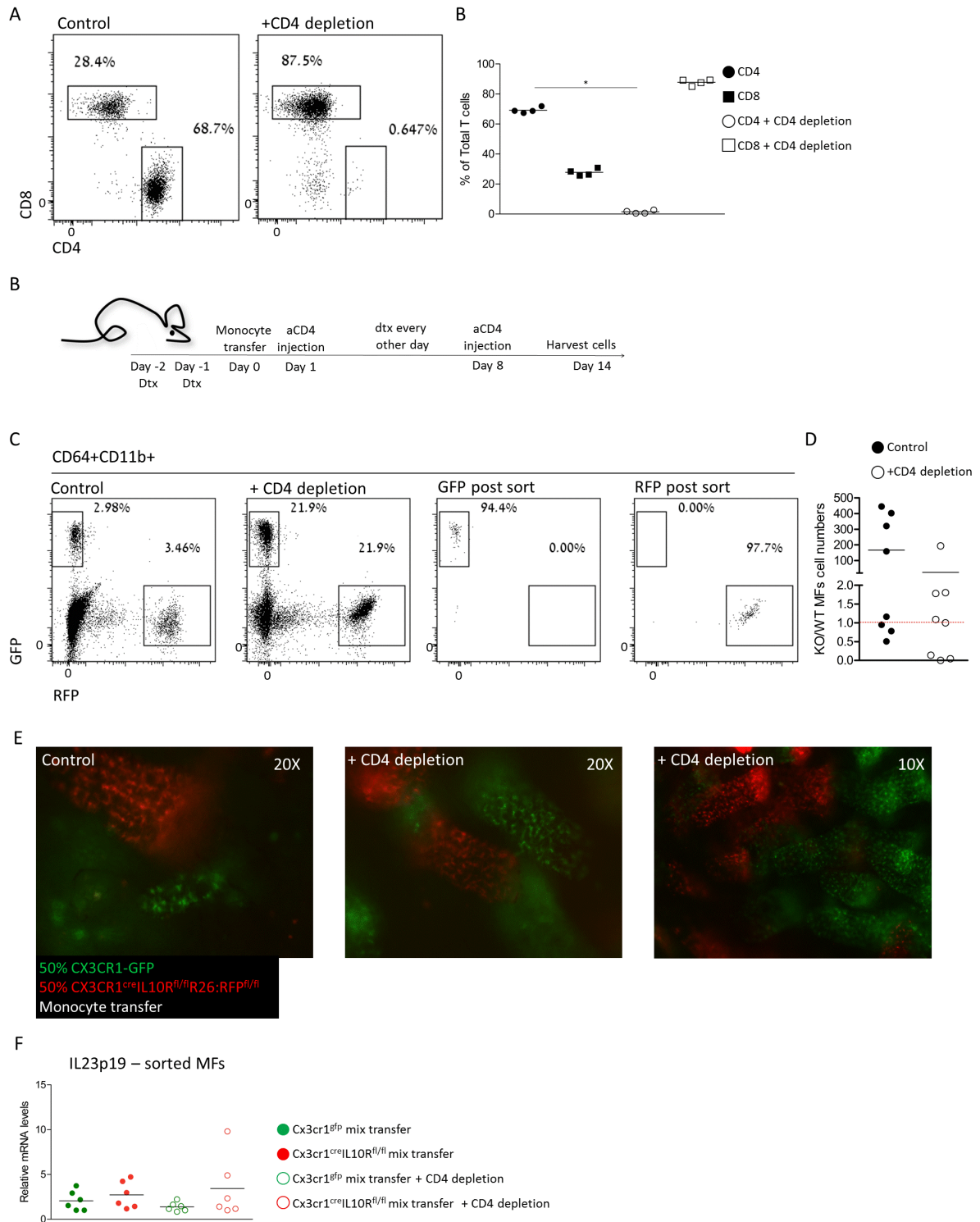


**Figure 15. CD4 depletion fails to release the pro-inflammatory phenotype of Il10 receptor**

**deficient macrophages (A)** FACS analysis of cells extracted from the mesenteric lymph node of mice treated with cd4 depleting antibody **(B)** Quantification of T cell numbers following CD4 T cell depletion **(C)** Experimental design of monocyte transfer with CD4 T cell depletion **(D)** FACS analysis of colonic lamina propria of mix monocyte transferred Cx3cr1<sup>dtr</sup> mice two weeks after cell transfer **(E)** Ratio of Il10r KO/WT macrophage numbers extracted from the colonic lamina propria of mix transferred mice **(F)** Live tissue imaging of the small intestine of mix monocyte transferred mice **(G)** qRT-PCR of RNA extracted from macrophages sorted from the colonic lamina propria of indicated mice, data pooled from two independent experiments, n>3 in each

## Discussion – part 2

Intestinal macrophages are monocyte derived, and depend on a constant flux of monocytes egressing from the BM and arriving to the intestinal tissue<sup>20,21</sup>. This allows us to study their differentiation using a monocyte transfer system. In this system we ablate the endogenous macrophage compartment of mice, and transfer monocytes of interest, which can be fluorescently labeled, or deficient for a specific gene, to track their differentiation and influence on the tissue. Furthermore, we are able to mix transfer the ablated mice to create a chimeric gut macrophage population. However, Il10r deficient macrophages in the transfer system failed to display any pro-inflammatory profile.

We examined several possible reasons for this failure:

- (1) The type of depletion system used and its influence on the tissue – we disproved this option since we tested macrophages differentiated in both a broad depleting system (CD11c-DTR) and a more specific depleting system (*Cx3cr1<sup>DTR</sup>*).
- (2) The time frame of differentiation is sufficient for the macrophages since in the BM chimera model, upon transfer of *Cx3cr1<sup>cre</sup>:Il10r<sup>fl/fl</sup>* BM to wt irradiated mice, two weeks are sufficient to develop a pro-inflammatory signature, including il23p19 expression by the cells, and AMP up-regulation by epithelial cells, indicating a response of the environment to pro-inflammatory macrophages.
- (3) Side effects of the DTx injections – first, the DTx injection is critical since without repeated injections the numbers of differentiated cells in the tissue were strongly reduced. Additionally, in colonic tissue of Il10r ko transferred *Cx3cr1<sup>DTR</sup>* mice, which were left without toxin treatment, there was no up regulation of AMPs in the tissue, and no Il23p19 production by transferred macrophages.
- (4) Epithelial permeability due to irradiation of BM chimeras – the difference we observe between the monocyte transfer system and the BM chimera system can be explained by the irradiation that BM chimeras receive prior to injection of the transferred BM. We tested this possibility by sub-lethally irradiating *Cx3cr1<sup>DTR</sup>* mice prior to monocyte transfer. However,

we did not find a difference between macrophages harvested from irradiated and non-irradiated mice.

- (5) An Il10 independent mechanism of macrophage regulation – it is possible that Il10 signaling is not an exclusive pathway to control macrophage activation. To address this possibility we depleted CD4 T cells during monocyte differentiation, since the cells which control macrophages are primarily Tregs. Again, we did not witness a difference in Il23p19 transcription levels between WT and Il10r deficient macrophages harvested from control or CD4 depleted monocyte transferred animals.

In conclusion, the monocyte transfer system so far did not allow us to study the differentiation of Il10r deficient macrophages, since we could not achieve an appropriate condition for the cells to exhibit their pro-inflammatory phenotype, as we witnessed in *Cx3cr1<sup>cre</sup>:Il10ra<sup>fl/fl</sup>* mice or BM chimeras. Further investigation is required to determine whether the graft-derived macrophages in the monocyte transfer system truly represent the heterogeneous population of intestinal macrophages.

Table 2 – Mouse strains used in Part 2:

Strain name	Knocked in/transgenes	Experiment
<i>Cx3cr1<sup>cre</sup>:Il10ra<sup>fl/fl</sup>:R26Rfp<sup>fl/fl</sup></i>	Cre recombinase Floxed <i>Il10r</i> allele Floxed <i>R26-RFP</i> allele	Monocyte transfer – donors of monocytes
<i>Cx3cr1<sup>slp/+</sup></i>	GFP	
<i>Cx3cr1<sup>DTR</sup></i> >WT BM chimera	DTR	Monocyte transfer
CD11c-DTR > WT BM chimera	DTR	

## Materials and methods

### Mice

All animals were on C57Bl/6 background and bred at the Weizmann animal facility. Age matched co housed males were used for all experiments. Animals were maintained under specific pathogen-free conditions and handled according to protocols approved by the Weizmann Institute Animal Care Committee as per international guidelines.

Cx3cr1<sup>DTR</sup> mice were generated by crossing Cx3cr1<sup>stop-DTR</sup> (Jackson stock number 025629 ) to Pgc1-Cre (Jackson stock number 020811). The progeny express DTR in all Cx3cr1 expressing cells.

Mouse strain	Jackson stock number
Cx3cr1 <sup>GFP</sup>	005582
Cd11c-DTR	004509

### Cell isolation, flow cytometry analysis and sorting of intestinal macrophages and intestinal epithelial cells

For the isolation of colonic EC, extra-intestinal fat tissue and blood vessels were carefully removed and colons were then flushed of their luminal content with cold PBS, opened longitudinally, and cut into 0.5 cm pieces. Colon pieces were incubated in RPMI medium supplemented with 2mM EDTA, 10%FBS, 1% PenStrep and 1% Sodium pyruvate for 40 minutes at 37°C shaking at 250 rpm.

For the isolation of colonic lamina propria cells, EC and mucus were removed by 40 min incubation with HBSS (without Ca<sup>2+</sup> and Mg<sup>2+</sup>) containing 5% FBS, 2 mM EDTA, and 0.15 mg/ml (1 mM) DTT (Sigma) at 37°C shaking at 250 rpm. Colon pieces were then digested in PBS<sup>+/+</sup> containing 5% FBS,

1 mg/ml Collagenase VIII (Sigma), and 0.1 mg/ml DNase I (Roche) for 40 min at 37°C shaking at 250 rpm. The digested cell suspension was then washed with PBS and passed sequentially through 100 and 40 mm cell strainers. Antibodies were used to stain the surface markers of the cells: CD45 (30-F11), Ly-6C (HK1.4), CD11b (M1/70), CD11c (HL3), Ly6G (1A8), CD64 (X54-5/7.1) from Biolegend, Bio-gems or eBioscience, CD103 (M290) from BD biosciences were used. Cells were

analyzed with LSRFortessa flow cytometer (BD) or sorted using a FACS Aria machine (BD). Flow cytometry analysis was done with the FlowJo software.

### Real time PCR

Total RNA was extracted from sorted cells with RNeasy Micro Kit (Qiagen) and from murine colons with PerfectPure RNA Tissue Kit (5 PRIME). RNA was reverse transcribed with a mixture of random primers and oligo-dT with a High-Capacity cDNA Reverse Transcription Kit (Applied Biosystems). PCR was performed with SYBR Green PCR Master Mix kit (Applied Biosystems). Quantification of the PCR signals of each sample was performed by comparing the cycle threshold values (Ct), in duplicate, of the gene of interest with the Ct values of the TATA-binding protein (TBP) housekeeping gene (for whole tissue RNA) or Actin-b (for sorted cells).

Primers used for qPCR:

Gene	Fw (5'→3')	Rev (5'→3')
Actb	GGAGGGGGTTGAGGTGTT	TGTGCACTTTTATTGGTCTCA
TBP	GAAGCTGCGGTACAATTCCAG	CCCCTTGTACCCTTCACCAAT
Reg3b	ACTCCCTGAAGAATATACCCTCC	CGCTATTGAGCACAGATACGAG
Reg3g	ATGCTTCCCCGTATAACCATCA	GGCCATATCTGCATCATAACCAG
Nos2	CTGCAGCACTTGGATCAGGAACCTG	GGGAGTAGCCTGTGTGCACCTGGAA
Il22	ATGAGTTTTTCCCTTATGGGGAC	GCTGGAAGTTGGACACCTCAA
Il23	ATGCTGGATTGCAGAGCAGTA	ACGGGGCACATTATTTTTAGTCT
Ccl5	AGATCTCTGCAGCTGCCCTCA	GGAGCACTTGCTGCTGGTGTAG
Cxcl5	TGCGTTGTGTTTGGCTTAACCG	CTTCCACCGTAGGGCACTG
Cxcl1	GACCATGGCTGGGATTCACC	GTGTGGCTATGACTTCGGTT

### Cell isolation, sorting and monocyte transfer

Bone marrow cells were harvested from the femora and tibiae of *Cx3cr1gfp/+ CD45.1* or *CX3CR1<sup>cre</sup> IL10R<sup>fl/fl</sup> RFP<sup>fl/fl</sup> CD45.2* mice and enriched for mononuclear cells on a Ficoll density gradient. Cells were isolated by either MACS cell separation or Fluorescence Activated Cell Sorting (FACS). For MACS separation, cells were incubated with CD115-biotin (AFS98 Biolegend) and streptavidin-conjugated magnetic beads (Miltenyi). For FACS, Ly6C<sup>hi</sup> monocytes were sorted by gating on cells positive for CD115 (AFS98 Biolegend), CD11b, and Ly6c and negative for CD117 (2B8 biolegend). In both cases, sorted monocytes were transferred intravenously to CD11c-dtr or *Cx3cr1<sup>DTR</sup>* bone marrow chimeras treated with 10ng/g

diphtheria toxin (Sigma-aldrich) one day prior to transfer, and every other day for the following 14 days.

### **RNA sequencing and analysis**

EC RNA sequencing was conducted with the help of the INCPM unit at the Weizmann institute of science – total RNA was extracted from  $0.1-1 \times 10^6$  sorted cells with RNeasy Micro Kit (Qiagen). 100 ng of total RNA was processed using the TruSeq Stranded Total RNA HTSample Prep Kit (with Ribo-Zero Gold) of Illumina (RS-122-2303). Libraries were evaluated by Qubit and TapeStation. Sequencing libraries were constructed with barcodes to allow multiplexing of 24 samples ran on 3 lanes. ~20 million single-end 50-bp reads were sequenced per sample on Illumina HiSeq 2500 high output mode instrument.

Macrophages RNA was sequenced using MARSeq, as previously described (D. Varol et al., 2017). Briefly,  $10^4-10^5$  cells from each population were sorted into 50  $\mu$ l of lysis/binding buffer (Life Technologies). RNA was captured with 12  $\mu$ l of Dynabeads oligo(dT) (Life Technologies), washed, and eluted at 70°C with 10  $\mu$ l of 10 mM Tris-Cl (pH 7.5). ~5 million reads were sequenced per library.

In both cases gene expression levels were calculated using the HOMER software package (analyzeRepeats.pl rna mm9 -d <tagDir> -count exons -condenseGenes -strand + -raw). Normalization and differential expression analysis was done using the DESeq2 R-package.

### **Immunohistochemistry**

Tissues were fixed in 2% paraformaldehyde at 4°C and stained for CD3 (SP7,abcam) and GFP (polyclonal IgG ab6658 ,abcam) overnight in 4°C. Alexa-fluor 488-conjugated donkey anti-goat and Cy3-conjugated donkey anti-rabbit (Jackson ImmunoResearch) secondary antibodies were added for 1 hour. Nuclei were stained with Hoechst. Tissues were evaluated using an Olympus BX51 microscope, and image acquisition was conducted with the Olympus DP70 camera and DP-Manager software. Image merging and further analysis was conducted using Velocity software.

## **Antibiotics treatment**

For antibiotic treatment, mice were given a combination of vancomycin (0.5 g/l), ampicillin (1 g/l), kanamycin (1 g/l), and metronidazole (1 g/l) in their drinking water. All antibiotics were obtained from Sigma Aldrich.

## **References**

1. Abraham, C. & Cho, J. H. Inflammatory Bowel Disease. *N. Engl. J. Med.* **361**, 2066–2078 (2009).
2. Manolio, T. A. *et al.* Finding the missing heritability of complex diseases. *Nature* **461**, 747–753 (2009).
3. Huang, H. *et al.* Fine-mapping inflammatory bowel disease loci to single-variant resolution. *Nature* **547**, 173–178 (2017).
4. Maloy, K. J. & Powrie, F. Intestinal homeostasis and its breakdown in inflammatory bowel disease. *Nature* **474**, 298–306 (2011).
5. Okayasu, I. *et al.* A novel method in the induction of reliable experimental acute and chronic ulcerative colitis in mice. *Gastroenterology* **98**, 694–702 (1990).
6. Zigmond, E. *et al.* Ly6C<sup>hi</sup> monocytes in the inflamed colon give rise to proinflammatory effector cells and migratory antigen-presenting cells. *Immunity* **37**, 1076–90 (2012).
7. Powrie, F., Correa-Oliveira, R., Mauze, S. & Coffman, R. L. Regulatory interactions between CD45RB<sup>high</sup> and CD45RB<sup>low</sup> CD4<sup>+</sup> T cells are important for the balance between protective and pathogenic cell-mediated immunity. *J Exp Med* **179**, 589–600 (1994).
8. Powrie, F., Leach, M. W., Mauze, S., Caddie, L. B. & Coffman, R. L. Phenotypically distinct subsets of CD4<sup>+</sup> T cells induce or protect from chronic intestinal inflammation in C. B-17 *scid* mice. *Int. Immunol.* **5**, 1461–1471 (1993).
9. Uhlig, H. H. *et al.* Differential activity of IL-12 and IL-23 in mucosal and systemic innate immune pathology. *Immunity* **25**, 309–318 (2006).
10. Kühn, R., Löhler, J., Rennick, D., Rajewsky, K. & Müller, W. Interleukin-10-deficient mice develop chronic enterocolitis. *Cell* **75**, 263–74 (1993).
11. Hoshi, N. *et al.* MyD88 signalling in colonic mononuclear phagocytes drives colitis in IL-10-deficient mice. *Nat. Commun.* **3**, 1120 (2012).

12. Varol, C., Zigmund, E. & Jung, S. Securing the immune tightrope: mononuclear phagocytes in the intestinal lamina propria. *Nat. Rev. Immunol.* **10**, 415–426 (2010).
13. Joeris, T., Müller-Luda, K., Agace, W. W. & Mowat, A. M. Diversity and functions of intestinal mononuclear phagocytes. *Mucosal Immunol* **10**, 845–864 (2017).
14. Sonnenberg, G. F. & Artis, D. Innate lymphoid cells in the initiation, regulation and resolution of inflammation. *Nat Med* **21**, 698–708 (2015).
15. Mortha, A. *et al.* Microbiota-dependent crosstalk between macrophages and ILC3 promotes intestinal homeostasis. *Science* **343**, 1249288 (2014).
16. Blander, J. M., Longman, R. S., Iliev, I. D., Sonnenberg, G. F. & Artis, D. Regulation of inflammation by microbiota interactions with the host. *Nat. Immunol.* **18**, 851–860 (2017).
17. Peterson, L. W. & Artis, D. Intestinal epithelial cells: regulators of barrier function and immune homeostasis. *Nat. Rev. Immunol.* **14**, 141–153 (2014).
18. Varol, C., Mildner, A. & Jung, S. Macrophages: Development and Tissue Specialization. *Annu. Rev. Immunol.* **33**, 643–675 (2015).
19. Bogunovic, M. *et al.* Origin of the Lamina Propria Dendritic Cell Network. *Immunity* **31**, 513–525 (2009).
20. Varol, C. *et al.* Intestinal Lamina Propria Dendritic Cell Subsets Have Different Origin and Functions. *Immunity* **31**, 502–512 (2009).
21. Bain, C. C. *et al.* Constant replenishment from circulating monocytes maintains the macrophage pool in the intestine of adult mice. *Nat Immunol* **15**, 929–937 (2014).
22. Zigmund, E. & Jung, S. Intestinal macrophages: well educated exceptions from the rule. *Trends Immunol.* **34**, 162–168 (2013).
23. Mildner, A. & Jung, S. Development and Function of Dendritic Cell Subsets. *Immunity* **40**, 642–656 (2014).
24. Sun, C.-M. *et al.* Small intestine lamina propria dendritic cells promote de novo generation of Foxp3 T reg cells via retinoic acid. *J. Exp. Med.* **204**, 1775–85 (2007).
25. Coombes, J. L. *et al.* A functionally specialized population of mucosal CD103+ DCs induces Foxp3+ regulatory T cells via a TGF-beta and retinoic acid-dependent mechanism. *J. Exp. Med.* **204**, 1757–64 (2007).

26. Dong, C. Diversification of T-helper-cell lineages: finding the family root of IL-17-producing cells. *Nat. Rev. Immunol.* **6**, 329–334 (2006).
27. Steinman, L. A brief history of TH17, the first major revision in the TH1/TH2 hypothesis of T cell-mediated tissue damage. *Nat. Med.* **13**, 139–145 (2007).
28. Stockinger, B. & Omenetti, S. The dichotomous nature of T helper 17 cells. *Nat. Rev. Immunol.* **17**, 535–544 (2017).
29. Gaublomme, J. T. *et al.* Single-Cell Genomics Unveils Critical Regulators of Th17 Cell Pathogenicity. *Cell* **163**, 1400–1412 (2015).
30. Wang, C. *et al.* CD5L/AIM Regulates Lipid Biosynthesis and Restrains Th17 Cell Pathogenicity. *Cell* **163**, 1413–1427 (2015).
31. Franke, A. *et al.* Genome-wide meta-analysis increases to 71 the number of confirmed Crohn’s disease susceptibility loci. *Nat. Genet.* **42**, 1118–1125 (2010).
32. Jostins, L. *et al.* Host–microbe interactions have shaped the genetic architecture of inflammatory bowel disease. *Nature* **491**, 119–124 (2012).
33. Spits, H. *et al.* Innate lymphoid cells — a proposal for uniform nomenclature. *Nat. Rev. Immunol.* **13**, 145–149 (2013).
34. Buonocore, S. *et al.* Innate lymphoid cells drive interleukin-23-dependent innate intestinal pathology. *Nature* **464**, 1371–5 (2010).
35. Gallo, R. L. & Hooper, L. V. Epithelial antimicrobial defence of the skin and intestine. *Nat. Rev. Immunol.* **12**, 503–516 (2012).
36. Abreu, M. T. Toll-like receptor signalling in the intestinal epithelium: how bacterial recognition shapes intestinal function. *Nat Rev Immunol* **10**, 131–144 (2010).
37. McDole, J. R. *et al.* Goblet cells deliver luminal antigen to CD103+ dendritic cells in the small intestine. *Nature* **483**, 345–349 (2012).
38. Nikitas, G. *et al.* Transcytosis of *Listeria monocytogenes* across the intestinal barrier upon specific targeting of goblet cell accessible E-cadherin. *J. Exp. Med.* **208**, 2263–77 (2011).
39. Clevers, H. C. & Bevins, C. L. Paneth Cells: Maestros of the Small Intestinal Crypts. *Annu. Rev. Physiol.* **75**, 289–311 (2013).
40. Sato, T. *et al.* Paneth cells constitute the niche for Lgr5 stem cells in intestinal crypts. *Nature* **469**, 415–418 (2011).
41. Engelstoft, M. S., Egerod, K. L., Lund, M. L. & Schwartz, T. W.

- Enteroendocrine cell types revisited. *Curr. Opin. Pharmacol.* **13**, 912–921 (2013).
42. Ivanov, I. I. *et al.* Induction of Intestinal Th17 Cells by Segmented Filamentous Bacteria. *Cell* **139**, 485–498 (2009).
  43. Shouval, D. S. *et al.* Interleukin 10 receptor signaling: master regulator of intestinal mucosal homeostasis in mice and humans. *Adv. Immunol.* **122**, 177–210 (2014).
  44. Moore, K. W., de Waal Malefyt, R., Coffman, R. L. & O’Garra, A. I INTERLEUKIN -10 AND THE I NTERLEUKIN -10 R ECEPTOR. *Annu. Rev. Immunol.* **19**, 683–765 (2001).
  45. Glocker, E.-O. *et al.* Inflammatory Bowel Disease and Mutations Affecting the Interleukin-10 Receptor. *N. Engl. J. Med.* **361**, 2033–2045 (2009).
  46. Zigmund, E. *et al.* Macrophage-restricted interleukin-10 receptor deficiency, but not IL-10 deficiency, causes severe spontaneous colitis. *Immunity* **40**, 720–733 (2014).
  47. Rubtsov, Y. P. *et al.* Regulatory T Cell-Derived Interleukin-10 Limits Inflammation at Environmental Interfaces. *Immunity* **28**, 546–558 (2008).
  48. Yona, S. *et al.* Fate Mapping Reveals Origins and Dynamics of Monocytes and Tissue Macrophages under Homeostasis. *Immunity* **38**, 79–91 (2013).
  49. Pils, M. C. *et al.* Monocytes/macrophages and/or neutrophils are the target of IL-10 in the LPS endotoxemia model. *Eur. J. Immunol.* **40**, 443–448 (2010).
  50. Shouval, D. S. *et al.* Interleukin-10 Receptor Signaling in Innate Immune Cells Regulates Mucosal Immune Tolerance and Anti-Inflammatory Macrophage Function. *Immunity* **40**, 706–719 (2014).
  51. Langrish, C. L. *et al.* IL-12 and IL-23: master regulators of innate and adaptive immunity. *Immunol. Rev.* **202**, 96–105 (2004).
  52. Hue, S. *et al.* Interleukin-23 drives innate and T cell-mediated intestinal inflammation. *J Exp Med* **203**, 2473–2483 (2006).
  53. Kullberg, M. C. *et al.* IL-23 plays a key role in *Helicobacter hepaticus*-induced T cell-dependent colitis. *J Exp Med* **203**, 2485–2494 (2006).
  54. Arnold, I. C. *et al.* CD11c(+) monocyte/macrophages promote chronic *Helicobacter hepaticus*-induced intestinal inflammation through the production of IL-23. *Mucosal Immunol.* **9**, 352–63 (2016).
  55. Ahern, P. P. *et al.* Interleukin-23 drives intestinal inflammation through direct

- activity on T cells. *Immunity* **33**, 279–288 (2010).
56. Sugimoto, K. *et al.* IL-22 ameliorates intestinal inflammation in a mouse model of ulcerative colitis. *J Clin Invest* **118**, 534–544 (2008).
  57. Zindl, C. L. *et al.* IL-22-producing neutrophils contribute to antimicrobial defense and restitution of colonic epithelial integrity during colitis. *Proc Natl Acad Sci U S A* **110**, 12768–12773 (2013).
  58. Zenewicz, L. A. *et al.* Innate and adaptive interleukin-22 protects mice from inflammatory bowel disease. *Immunity* **29**, 947–957 (2008).
  59. Sabat, R., Ouyang, W. & Wolk, K. Therapeutic opportunities of the IL-22-IL-22R1 system. *Nat Rev Drug Discov* **13**, 21–38 (2014).
  60. Eken, A., Singh, A. K., Treuting, P. M. & Oukka, M. IL-23R<sup>+</sup> innate lymphoid cells induce colitis via interleukin-22-dependent mechanism. *Mucosal Immunol* **7**, 143–154 (2014).
  61. Huber, S. *et al.* IL-22BP is regulated by the inflammasome and modulates tumorigenesis in the intestine. *Nature* **491**, 259–63 (2012).
  62. Mantovani, A. & Marchesi, F. IL-10 and Macrophages Orchestrate Gut Homeostasis. *Immunity* **40**, 637–639 (2014).
  63. Duerr, R. H. *et al.* A genome-wide association study identifies IL23R as an inflammatory bowel disease gene. *Science (80-. )*. **314**, 1461–1463 (2006).
  64. Zheng, Y. *et al.* Interleukin-22, a TH17 cytokine, mediates IL-23-induced dermal inflammation and acanthosis. *Nature* **445**, 648–651 (2007).
  65. Zheng, Y. *et al.* Interleukin-22 mediates early host defense against attaching and effacing bacterial pathogens. *Nat. Med.* **14**, 282–289 (2008).
  66. Eberl, G. *et al.* An essential function for the nuclear receptor ROR $\gamma$ t in the generation of fetal lymphoid tissue inducer cells. *Nat. Immunol.* **5**, 64–73 (2004).
  67. Lochner, M. *et al.* In vivo equilibrium of proinflammatory IL-17<sup>+</sup> and regulatory IL-10<sup>+</sup> Foxp3<sup>+</sup> ROR $\gamma$ t<sup>+</sup> T cells. *J Exp Med* **205**, 1381–1393 (2008).
  68. Satoh-Takayama, N. *et al.* The Chemokine Receptor CXCR6 Controls the Functional Topography of Interleukin-22 Producing Intestinal Innate Lymphoid Cells. *Immunity* **41**, 776–788 (2014).
  69. Sonnenberg, G. F., Fouser, L. A. & Artis, D. Functional biology of the IL-22-IL-22R pathway in regulating immunity and inflammation at barrier surfaces.

- Adv. Immunol.* **107**, 1–29 (2010).
70. el Marjou, F. *et al.* Tissue-specific and inducible Cre-mediated recombination in the gut epithelium. *Genesis* **39**, 186–93 (2004).
  71. Hua, G. *et al.* Crypt Base Columnar Stem Cells in Small Intestines of Mice Are Radioresistant. *Gastroenterology* **143**, 1266–1276 (2012).
  72. Aychek, T. *et al.* IL-23-mediated mononuclear phagocyte crosstalk protects mice from *Citrobacter rodentium*-induced colon immunopathology. *Nat. Commun.* **6**, 6525 (2015).
  73. Kinnebrew, M. A. *et al.* Bacterial Flagellin Stimulates Toll- Like Receptor 5–Dependent Defense against Vancomycin- Resistant *Enterococcus* Infection. *J. Infect. Dis.* **201**, 534–543 (2010).
  74. Longman, R. S. *et al.* CX3CR1<sup>+</sup> mononuclear phagocytes support colitis-associated innate lymphoid cell production of IL-22. *J. Exp. Med.* **211**, 1571–83 (2014).
  75. Thakker, P. *et al.* IL-23 is critical in the induction but not in the effector phase of experimental autoimmune encephalomyelitis. *J. Immunol.* **178**, 2589–98 (2007).
  76. Redhu, N. S. *et al.* Macrophage dysfunction initiates colitis during weaning of infant mice lacking the interleukin-10 receptor. *Elife* **6**, (2017).
  77. Brooks, S. A. & Blackshear, P. J. Tristetraprolin (TTP): interactions with mRNA and proteins, and current thoughts on mechanisms of action. *Biochim. Biophys. Acta* **1829**, 666–79 (2013).
  78. Taylor, G. A. *et al.* A Pathogenetic Role for TNF $\alpha$  in the Syndrome of Cachexia, Arthritis, and Autoimmunity Resulting from Tristetraprolin (TTP) Deficiency. *Immunity* **4**, 445–454 (1996).
  79. Molle, C. *et al.* Tristetraprolin regulation of interleukin 23 mRNA stability prevents a spontaneous inflammatory disease. *J. Exp. Med.* **210**, 1675–84 (2013).
  80. Schaljo, B. *et al.* Tristetraprolin is required for full anti-inflammatory response of murine macrophages to IL-10. *J. Immunol.* **183**, 1197–206 (2009).
  81. Martin, C. *et al.* Chemokines Acting via CXCR2 and CXCR4 Control the Release of Neutrophils from the Bone Marrow and Their Return following Senescence. *Immunity* **19**, 583–593 (2003).
  82. Eash, K. J., Greenbaum, A. M., Gopalan, P. K. & Link, D. C. CXCR2 and

- CXCR4 antagonistically regulate neutrophil trafficking from murine bone marrow. *J. Clin. Invest.* **120**, 2423–31 (2010).
83. Joeris, T., Müller-Luda, K., Agace, W. W. & Mowat, A. M. Diversity and functions of intestinal mononuclear phagocytes. *Mucosal Immunol.* **10**, 845–864 (2017).
84. Schridde, A. *et al.* Tissue-specific differentiation of colonic macrophages requires TGF $\beta$  receptor-mediated signaling. *Mucosal Immunol.* (2017). doi:10.1038/mi.2016.142
85. Buonocore, S. *et al.* Innate lymphoid cells drive interleukin-23-dependent innate intestinal pathology. *Nature* **464**, 1371–1375 (2010).
86. Ma, H.-L. *et al.* IL-22 is required for Th17 cell-mediated pathology in a mouse model of psoriasis-like skin inflammation. *J. Clin. Invest.* **118**, 597–607 (2008).
87. Behnsen, J. *et al.* The Cytokine IL-22 Promotes Pathogen Colonization by Suppressing Related Commensal Bacteria. *Immunity* **40**, 262–273 (2014).
88. Feagan, B. G. *et al.* Ustekinumab as Induction and Maintenance Therapy for Crohn's Disease. *N. Engl. J. Med.* **375**, 1946–1960 (2016).
89. Sandborn, W. J. *et al.* Ustekinumab Induction and Maintenance Therapy in Refractory Crohn's Disease. *N. Engl. J. Med.* **367**, 1519–1528 (2012).
90. Seiderer, J. & Brand, S. IL-22: A Two-Headed Cytokine in IBD? *Inflamm. Bowel Dis.* **15**, 473–474 (2009).
91. Brand, S. *et al.* IL-22 is increased in active Crohn's disease and promotes proinflammatory gene expression and intestinal epithelial cell migration. *Am. J. Physiol. Liver Physiol.* **290**, G827–G838 (2006).
92. Andoh, A. *et al.* Interleukin-22, a Member of the IL-10 Subfamily, Induces Inflammatory Responses in Colonic Subepithelial Myofibroblasts. *Gastroenterology* **129**, 969–984 (2005).
93. Sonnenberg, G. F., Fouser, L. A. & Artis, D. in 1–29 (2010). doi:10.1016/B978-0-12-381300-8.00001-0
94. Wolk, K. *et al.* IL-22 Increases the Innate Immunity of Tissues. *Immunity* **21**, 241–254 (2004).
95. Ouyang, W. Distinct roles of IL-22 in human psoriasis and inflammatory bowel disease. *Cytokine Growth Factor Rev.* **21**, 435–441 (2010).
96. Sugimoto, K. *et al.* IL-22 ameliorates intestinal inflammation in a mouse model of ulcerative colitis. *J. Clin. Invest.* **118**, 534–44 (2008).

97. Mizoguchi, A. Healing of intestinal inflammation by IL-22. *Inflamm. Bowel Dis.* **18**, 1777–1784 (2012).
98. Liu, J. Z., Pezeshki, M. & Raffatellu, M. Th17 cytokines and host-pathogen interactions at the mucosa: Dichotomies of help and harm. *Cytokine* **48**, 156–160 (2009).
99. Raffatellu, M. *et al.* Lipocalin-2 Resistance Confers an Advantage to *Salmonella enterica* Serotype Typhimurium for Growth and Survival in the Inflamed Intestine. *Cell Host Microbe* **5**, 476–486 (2009).
100. Aujla, S. J. *et al.* IL-22 mediates mucosal host defense against Gram-negative bacterial pneumonia. *Nat. Med.* **14**, 275–281 (2008).
101. Aujla, S. J. & Kolls, J. K. IL-22: a critical mediator in mucosal host defense. *J Mol Med* **87**, 451–454 (2009).
102. Lavin, Y. *et al.* Tissue-resident macrophage enhancer landscapes are shaped by the local microenvironment. *Cell* **159**, 1312–26 (2014).
103. Bar-On, L. & Jung, S. in *Methods in molecular biology (Clifton, N.J.)* **595**, 429–442 (2010).
104. Curato, C., Bernshtein, B., Aychek, T. & Jung, S. In Vivo Analysis of Intestinal Mononuclear Phagocytes. *Methods Mol Biol* **1423**, 255–268 (2016).
105. Diehl, G. E. *et al.* Microbiota restricts trafficking of bacteria to mesenteric lymph nodes by CX(3)CR1(hi) cells. *Nature* **494**, 116–120 (2013).
106. Hebel, K. *et al.* Plasma cell differentiation in T-independent type 2 immune responses is independent of CD11chigh dendritic cells. *Eur. J. Immunol.* **36**, 2912–2919 (2006).
107. Christensen, A. D., Skov, S., Kvist, P. H. & Haase, C. Depletion of regulatory T cells in a hapten-induced inflammation model results in prolonged and increased inflammation driven by T cells. *Clin. Exp. Immunol.* **179**, 485–499 (2015).